DNMI DET NORSKE METEOROLOGISKE INSTITUTT

klima

Trends and variability in North European pressure series

Ole Einar Tveito

REPORT NO. 27/96 KLIMA

DNMI-REPORT

NORWEGIAN METEOROLOGICAL INSTITUTE
P.O. BOX 43 BLINDERN, N - 0313 OSLO
TELEPHONE: (+47) 22 96 30 00

ISBN 0805-9918

REPORT NO.
27/96 KLIMA

DATE
29.08.96

TITLE

Trends and variability in North Atlantic pressure series.

AUTHOR

Ole Einar Tveito

PROJECT CONTRACTOR

Norwegian Meteorological Institute (DNMI)

SUMMARY

The mean level pressure series of the North Atlantic Climatological Dataset (NACD) was examined for temporal and spatial variability. Two periods were studied; 1921-1990 so the Arctic region was represented, and 1893-1990.

The series were analyzed using two approaches. In the first approach the dataseries were smoothed using Gauss filter-technique. The resulting series were compared, and groups were formed based on the shape of the smoothed curves. Eight groups were established. Analysis of correlation between the series in subperiods of 20 years showed large variations in correlation between the different groups in different periods.

The second approach was the method of empirical orthogonal functions (EOF). The results applying this method gave results similar to the smoothed curves.

Four gradients were also analyzed to examine the zonal and meridional winds in the study area. This examination showed that trends occur in these gradient series. In Western Norway are large correlations between zonal component and precipitation.

SIGNATURES

Ole Einar Tveito
RESEARCH SCIENTIST

Bjørn Aune
HEAD OF DIVISION

CONTENTS

1. INTRODUCTION

Pressure patterns are important for explaining the variability of other climatological elements like temperature and precipitation. To establish relations between large scale circulation and local climatology, for example for downscaling of GCM-results, these patterns have to be studied.

The North Atlantic Climatological Dataset (NACD) (Frich et.al, 1996) consists of long high quality climate dataseries from 9 North European countries. One of the aims in the NACD-project was to map the variability of the different climatological elements with respect to both time and space. Analysis on temperature (Hanssen-Bauer et.al, 1996) and precipitation (Førland et.al, 1996) indicates variations in the pressure patterns as a source to the variations found for these two elements. This report present the results of an introductory study to the variability of air pressure series in the north-Atlantic region during the last century.

In this investigation trend analysis and empirical orthogonal functions (EOF) are used to examine the temporal and spatial trends in pressure series.

2. DATA

The data used in this examination are the series of mean sea level air pressure from the North Atlantic Climate Dataset (NACD) (Frich et.al, 1996). This dataset covers the north Atlantic area for the period 1890 to 1990. For this analysis the period 1921-90 was chosen as the primary period, including at least one arctic station in the material. As a supplement, the period 1893 to 1990 was analysed, to check the variability also in the first 30 years of the series.

Only series with complete records were accepted in the analysis, due to the EOF-analysis. 31 of the NACD series fulfilled this criterion for the period 1921-90, 25 for the period 1893-90.

The locations of the NACD pressure series are shown in figure 2.1, the series used in this investigation have filled markers. Table 2.1 show a list of the series.

Table 2.1 NACD pressure series:

stnr	name	stnr	name
6447	UCCLE	1026	TROMSØ
6193	HAMMERODDE FYR	1028	BJØRNØYA
21100	VESTERVIG	1065	KARASJOK
25140	NORDBY	1098	VARDØ
304	HELSINKI	1100	SHIP "M"
5404	OULU	1152	BODØ
7501	SODANKYLÄ	1212	ONA
6011	TORSHAVN	1235	KJØREMSGRENDI/DOMBÅS
4210	UPERNAVIK	1271	VÆRNES/TRONDHEIM
4216	JAKOBSHAVN	1316	BERGEN-FLORIDA
4250	GODTHÅB	1355	LÆRDAL
4270	IVIGTUT/NARSARSUAQ	1403	UTSIRA FYR
4320	DANMARKSHAVN	1448	OKSØY FYR
4339	SCORESBYSUND	1482	FERDER FYR
4360	AMMASALIK	1492	OSLO-BLINDERN
44	LERWICK	6235	DE KOOY
293	WICK	6260	DE BILT
425	STORNOWAY	6280	EELDE
3953	VALENTIA OBS.	6310	VLISSINGEN
4013	STYKKISHOLMUR	6380	MAASTRICHT
4030	REYKJAVIK	6641	KALMAR
4048	VESTMANNAEYJAR	7243	GÖTEBORG
4063	AKUREYRI	7839	VISBY
4092	TEIGARHORN	9752	UPPSALA
1001	JAN MAYEN	12738	HÄRNÖSAND
1008	SVALBARD LUFTHAVN	16395	HAPARANDA

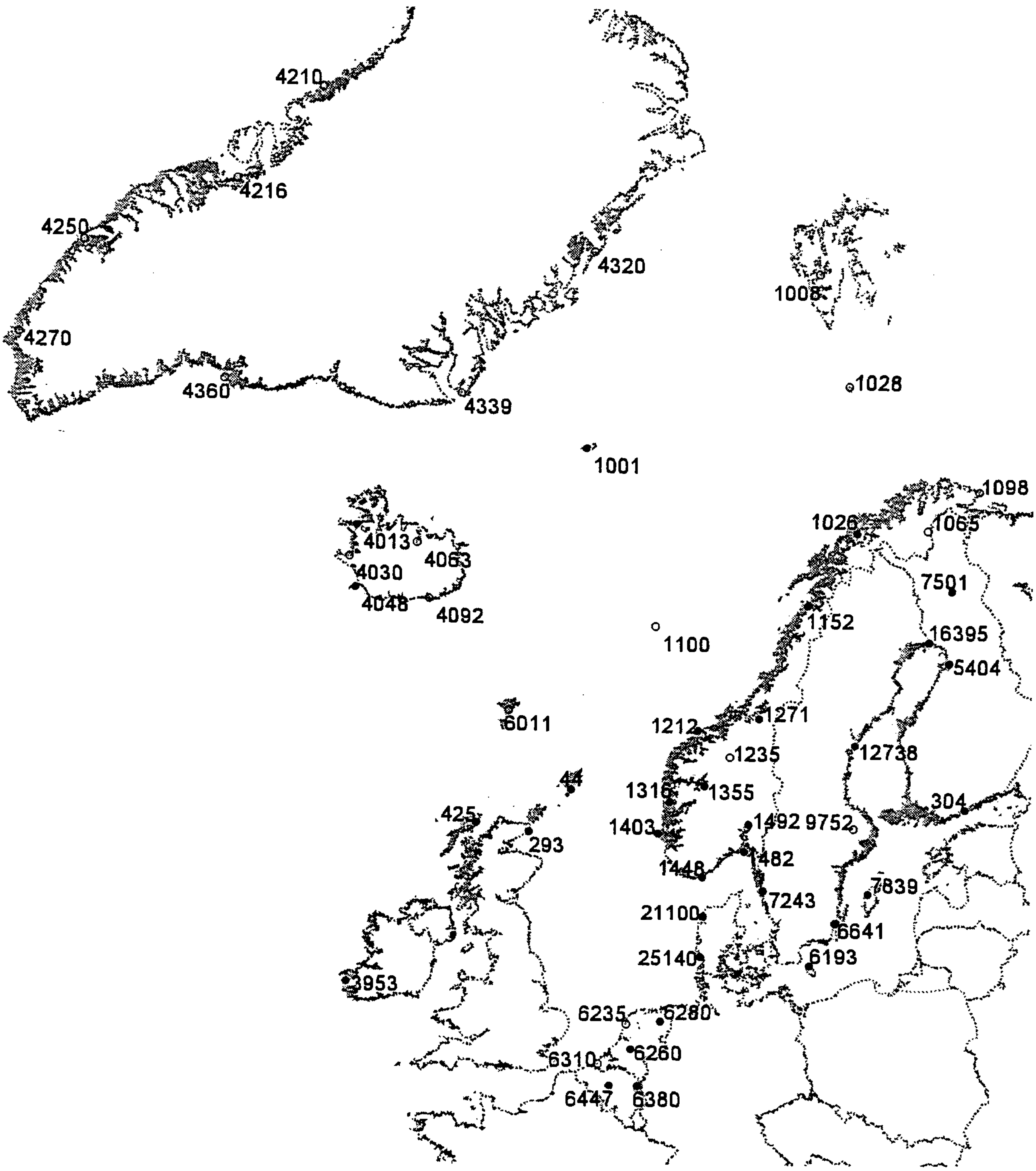

Figure 2.1 Location of the NACD pressure series, filled markers shows series used in this analysis.

3. TREND SERIES ANALYSIS

3.1 Comparison of trend series, 1921-90.

This analysis follows the principle of comparative trends presented by Hanssen-Bauer et.al. (1996b), examining standardized filtered time series. Only annual series were studied.

The series was standardized by dividing each of the individual years by the mean of the total period. This was done to reduce the series to the same level, and thereby gain a better basis for comparison of the series.

The series were filtered using Gauss filter technique (Alexandersson and Eriksson, 1989), with filter length 9 standard deviations, representing filter width of approximately 30 years. The resulting filtered series are shown in figure 3.1. A code was attached to each series, describing whether the series is increasing (+), decreasing (-) or constant (0) within a decade. Series showing similar patterns were grouped together. For mean annual pressure values, eight groups were formed (figure 3.2). Regional trends can be estimated as the mean of the series included in the region. Figure 3.3 show the regional curves. The thick lines are the regional curves, and the thin lines are the individual series grouped in this region.

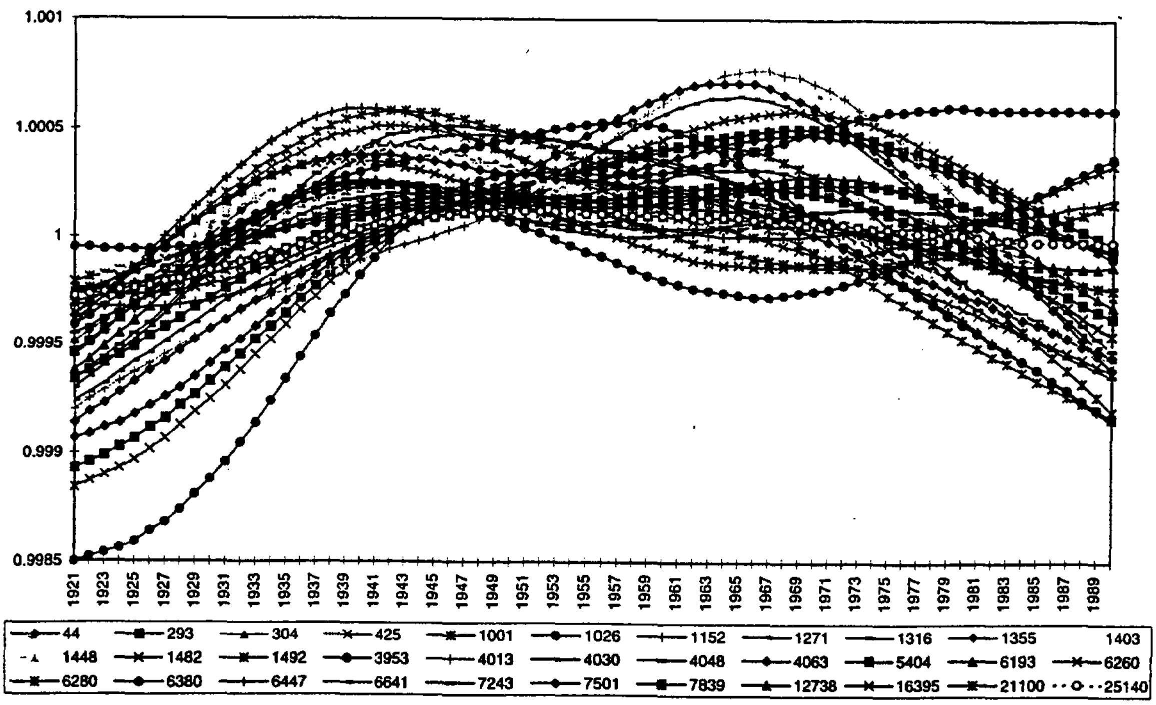

Figure 3.1 Filtered NACD pressure series 1921-90. Filter length 9σ.

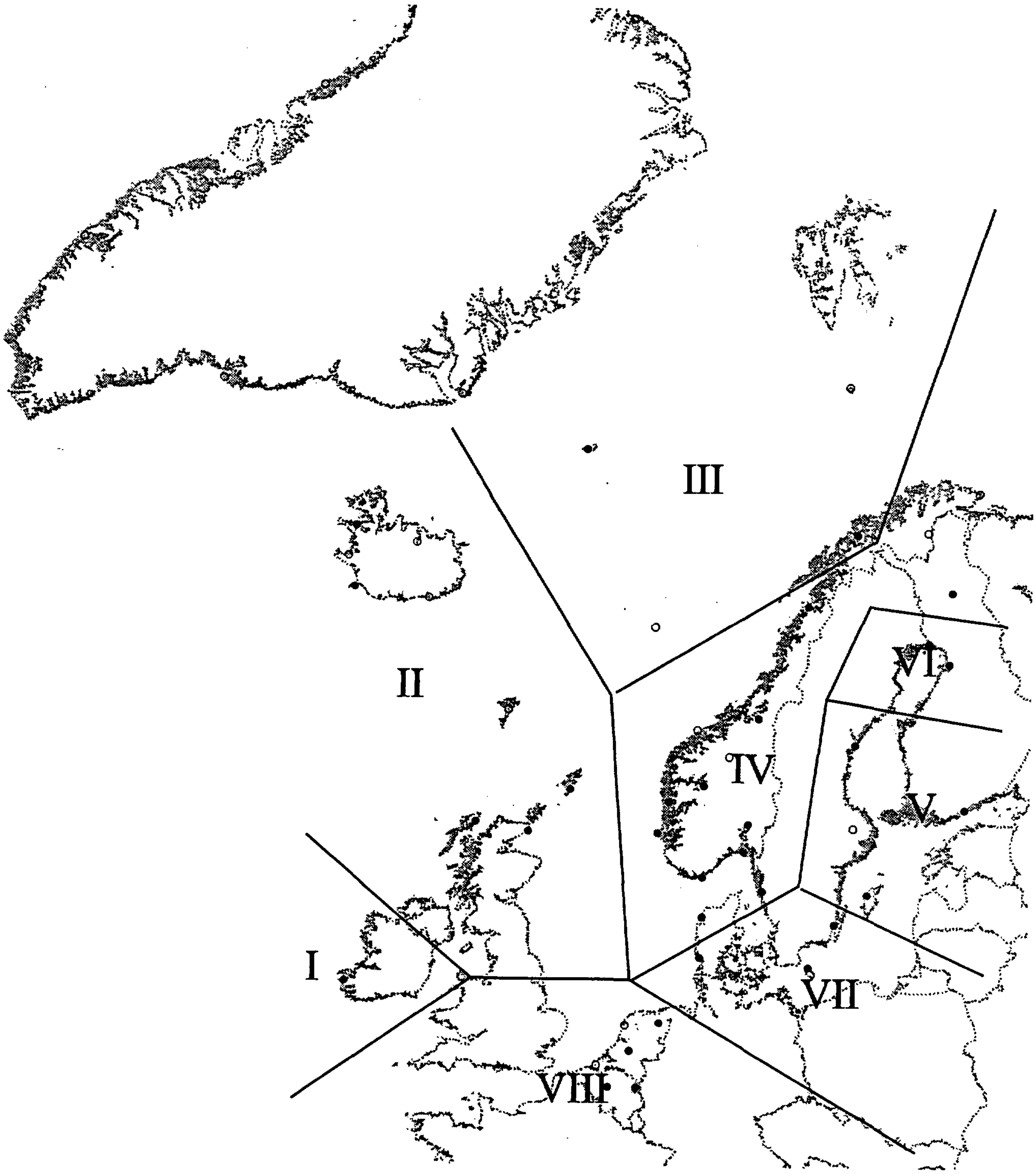

Figure 3.2 Pressure regions.

Group I (fig. 3.3a) consists of one series only, the Irish series of Valentia Observatory. This series increases rapidly the three first decades (1921-50), is constant the next ten years. In the period 1960-1975 the series increases weakly, and is almost constant for the last 15 years.

Group II (fig. 3.3b) consists of the series of Scotland, Orkneys, Shetland and Iceland. In this group there is an increase until 1965, and a decrease the remaining 25 years or so. The series 04048 Vestmannaeyjar deviates from the general patterns. It is relatively flat from 1940 to 1965, with a little "bump" around 1950.

Group III (fig. 3.3c) consists of two series, Jan Mayen and Tromsø, and represents the Norwegian Sea. The group shows the same patterns as group II, but the variation range is smaller. Note the different turningpoints of the two series, and the also the different pattern of the series 1026 Tromsø in the first part of the period compared to the 1001 Jan Mayen series. The series of Tromsø has similarities with the series of group IV.

Group IV (fig. 3.3d) is covering Norway, northern parts of Finland, northwestern parts of Sweden and northwest Jutland (Denmark). This group is characterized by an increase until 1940-50. The series of Bergen (1316), Trondheim (1271) and Vestervig (21100) deviates a little bit from the others, having a later turning point.

Group V (fig 3.3e) covers the area of southern Finland and eastern parts of Sweden. In this group there is an increase until around 1940, then a decrease until about 1955. After that a new increase until ~1970 occur, followed by a decrease the remainder of the period. The series of Kalmar (6641) deviates in the last part of the period, with a less marked decrease.

Group VI (fig 3.3f) is a transition group between group IV and V, covering mid-Finland. The series of Haparanda (16395) follows the pattern of the Norwegian group (IV), but the decrease in the period 1960-75 is somewhat weaker.

Group VII (fig 3.3g) is the south-Scandinavian group, covering most of Denmark and the southern parts of Sweden. There is an increase until 1960, and a decrease in the remaining years.

The last group, group VIII (fig 3.3h) consists of the series from the Netherlands and Belgium. They are constant the first years. After that they climb until around 1948.

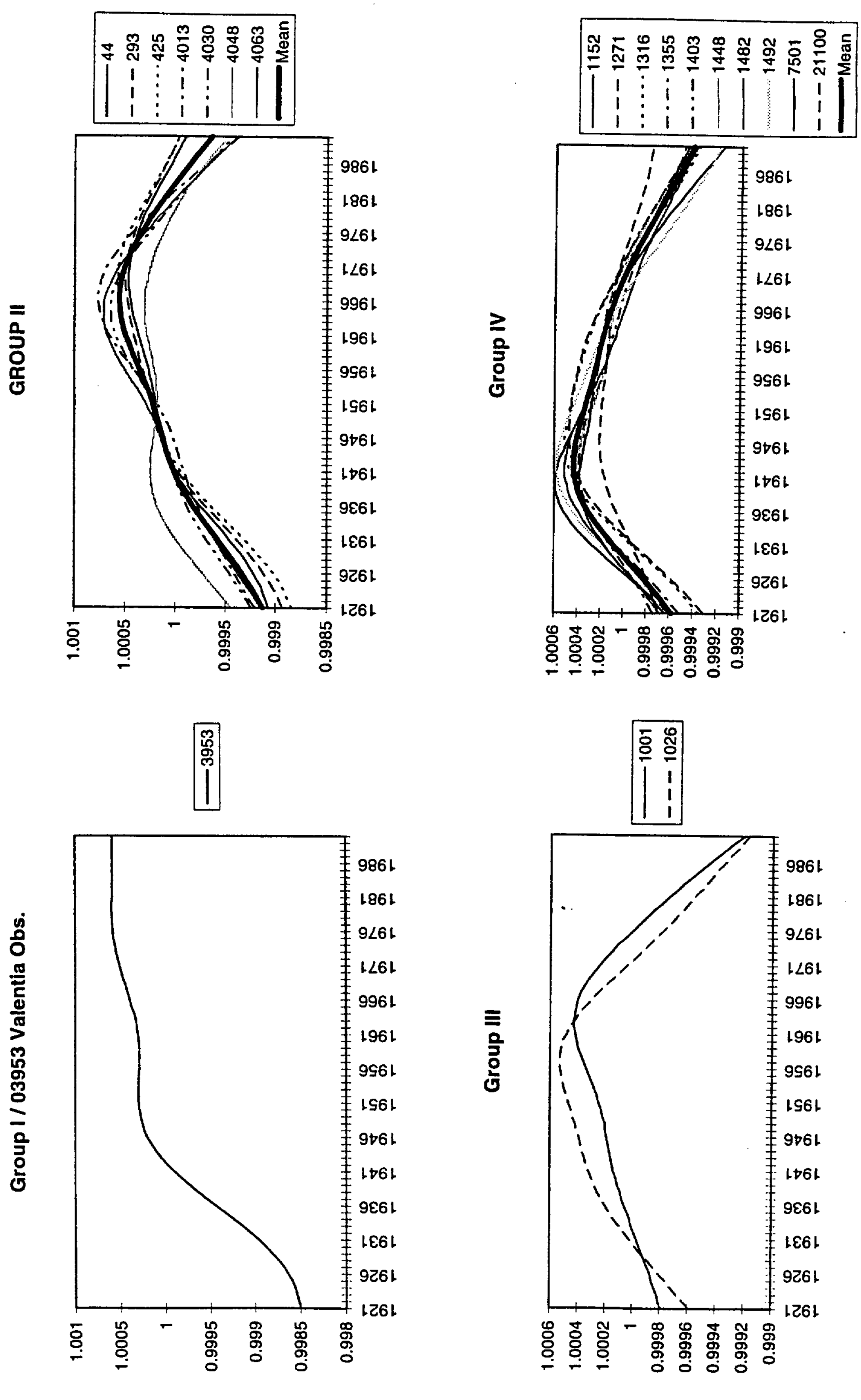

Figure 3.3 Regional trendcurves.

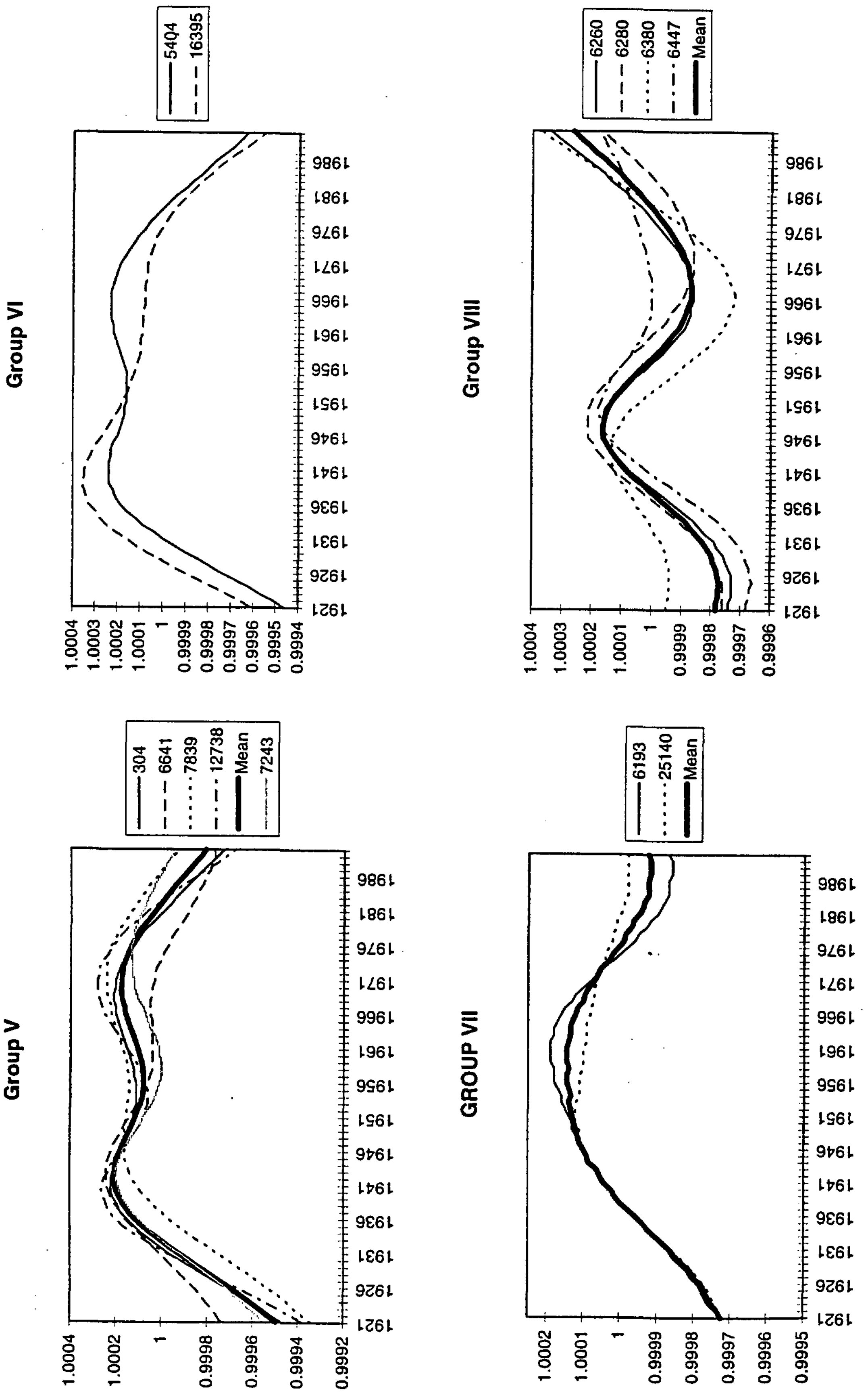

Figure 3.3 Regional trend curves - continued.

Then there is a decrease until the late sixties, before an increase the remaining part of the period.

This classification of the series is quite rough, and may be questioned. Uncertainties connected to this rather subjective approach are:

- Mirror effects in the filter. Interpretation of the filtered series close to the ends should be made very carefully, since the original values are given double weight. Extreme values in the tails will therefore dominate disproportionately.
- Station coverage is sparse in certain areas. Areas with few series can only give indications of regional behaviour.
- Inconsistency throughout the period. Some stations within a group can belong to different regimes within the 70 years studied.

Some groups have very similar patterns, e.g., group II and III, and group V and VI. Joining these groups has been evaluated. The patterns of the different groups are though so different that this is not recommended. In the case of group II and III the variations are much larger in group II. The increase is weaker in group III than in group II, and the decrease starts some years earlier. In the case of group V and VI, the decrease in group VI starts earlier. The decrease is also stronger.

3.2 Trend series, correlation analysis.

The correlation between the series was calculated, both for the whole period and for moving twenty year periods. There was a 10-year step between the periods. The results were organized as correlation matrixes, and the order of the series was grouped into the regions established from the comparison of trends.

The analysis showed large variations in the correlation matrix between the periods.

The correlation matrixes were plotted as grids (figure 3.4), given colours representing correlation values. This colourful "art" is an easy way to visualize the results, but rather complex to interpret. Red colour represents high positive correlation between series in the matrix, yellow indicates large negative correlation.

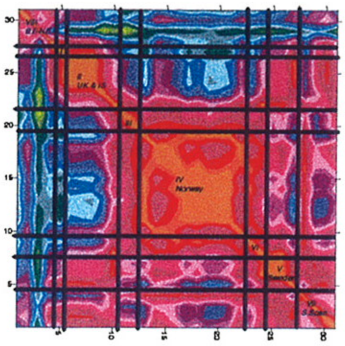

a) 1921-90

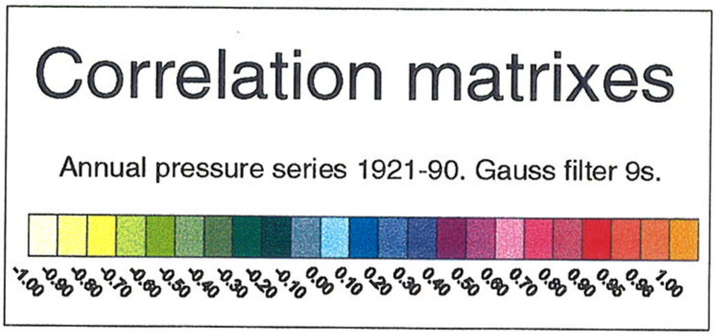

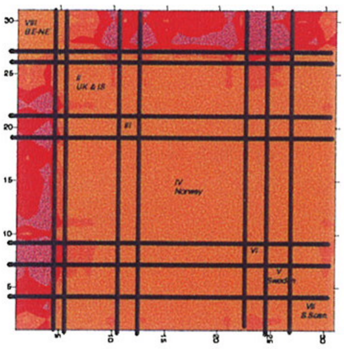

b) 1921-40

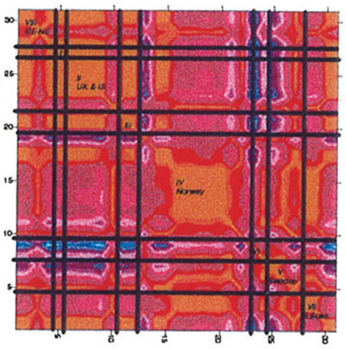

c) 1931-50

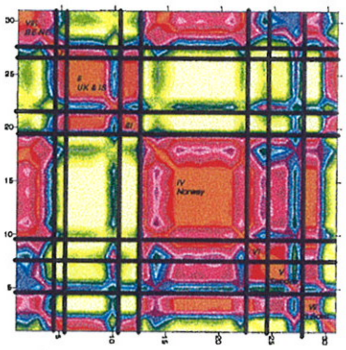

d) 1941-60

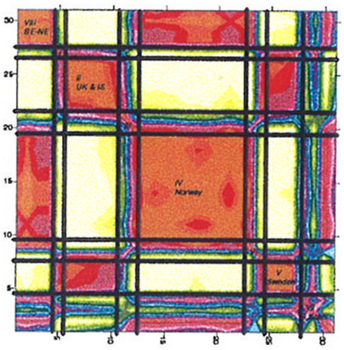

e) 1951-70

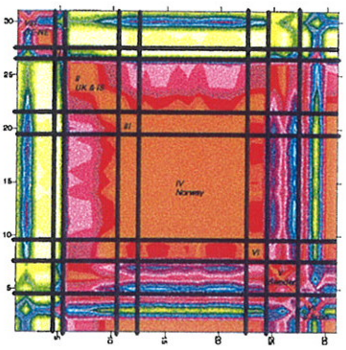

f) 1961-80

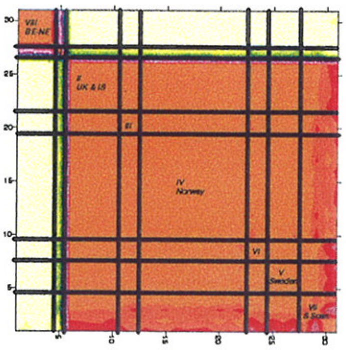

g) 1971-90

Figure 3.4 Correlation matrixes of filtered series 1921-90.

For the total period 1921-90 (fig 3.4a) most of the series are positively correlated. The series 6380 Maastricht is the only one deviating, this series has in large periods the opposite trends than most of the other series. The other series in group VIII have the same major characteristics, but not as extreme as the Maastricht series. Series 10 in the matrix, 4048 Vestmanneyjar of Iceland has much of the same patterns as the Scandinavian series.

All the series are highly correlated in the period 1921-40 (figure 3.4b). The uniform picture of this period can be a result of the mirror effect in the filtering technique. Most of the series are increasing in this period.

The pattern of the next period (1931-50, figure 3.4c) is more variable. In this period there are some changes in the trends. The series deviating is the series of 1152 Bodø (Norway) and 16395 Haparanda (Sweden), and to some extent 12738 Härnösand (Sweden). These three series have a change from a positive to a negative trend within the period, somewhat earlier than the majority of the series.

Figure 3.4d shows the period 1941-60. In group II the series 4048 still deviates. What characterizes this period is the contrary behaviour of the UK, Iceland and Atlantic (group II and III) series compared to most Scandinavian and continental series. The series of group II and III do not reach their turning points until the sixties.

The period 1951-70 gives the same picture (figure 3.4e), but even more clearly. In group III the series are not very correlated in this period, reflecting the different turning points of Jan Mayen and Tromsø. The same effect is found in group VI, where 5404 Oulu has an increase, while 16395 Haparanda is slowly decreasing. It is also interesting to see the difference between group IV and group V.

In the period 1961-80 are the Irish (group I) and Belgian-Dutch (group VIII) series negatively correlated to the rest of the groups (figure 3.4f). The series 7230 Gothenburg (series nr. 29 along the abscissa) is a little different from the other Scandinavian series.

The last period (1971-90, figure 3.4f) has a uniform pattern. As for the period 1921-40 much of the uniformity can be explained by the mirror effect.

What do the results of the correlation analysis indicate? They show that the pressure have the same patterns, an increase in pressure, for the entire region in the first part of the studied period. From ~1940 there seem to be a gradual change until ~1970. The difference occurs first between the western and eastern groups. The western groups include group I, II and III. These groups have the last turnover of all groups, in the period 1955-70. It is also interesting to look at the opposite trends of the southern parts (group I and group VIII). Group I has changed from following the Scottish and Icelandic series to follow the European series of Belgium and the Netherlands.

The results do also show that the pressure pattern over northern Europe is not constant, but large variations occur. These variations occur both temporarily and spatially.

3.3 The period 1893-1990.

The period 1893 to 1990 was also examined. For this period, 25 series were available. Standardization was made by using the 1893-1990 mean. As seen in figure 3.5 (filtered series, all 25) most of the series have little variation, or a weak decrease in the first 30 years of the period. One exception is the series of Valentia Observatory in Ireland, which has a very rapid decrease from 1893 to around 1915. Then it increases as described in section 3.1 from around 1920.

The series of group II splits. The British series is weakly increasing all the way, except Stornoway (425), which has a constant level from 1913-1924. There is an increase in the Icelandic series, like most of the others, the first 25-30 years. There are similarities between 4013 Stykkisholmur and 425 Stornoway.

In Norway some differences between different areas occur in the period 1893-1920. Most of the series has a marked decrease in pressure in this period. The decrease is strongest in the western series, less marked in south east (1482 and 1492), and almost not present in the northern series.

The series of Gothenburg and Denmark have the same patterns as the series of southeast Norway, a decrease until 1917. 25140 Nordby has a weaker decrease than the others.

In the series around the Baltic Sea there are two different patterns. The Swedish series of Härnösand have a decrease until 1927, like the Belgian series 6447. The series in the southern parts are quite flat, with a weak decrease until 1917-19. In the other series, like the Finnish, the same patterns as the Norwegian series are present, a decrease until 1917-19.

3.4 Mann-Kendall test on annual values, 1893-1990.

To check the significance of the trends, Mann-Kendall test (Hanssen-Bauer et.al, 1996) was performed on annual values for all 25 series covering the period 1893-90. The results reveal large differences concerning trends in the study area. The general tendencies found from the examination of the smoothed trend curves are also found with respect to regionality. Plotting the series of the Mann-Kendall statistics (Appendix A), with the 1% and 5% significance level, make detections of significant trends easy. The test was performed both forward and backward, starting in 1893 and 1990 respectively. This is done, since the level of the first value in the series will influence on the trend statistics.

The series of Valentia Observatory has significant trends. First a negative trend until 1917, then a positive trend. Both trends are significant on the 1% level for the forward test. The backward test indicates no trend until 1937, when a strong negative trend occur (backwards in time).

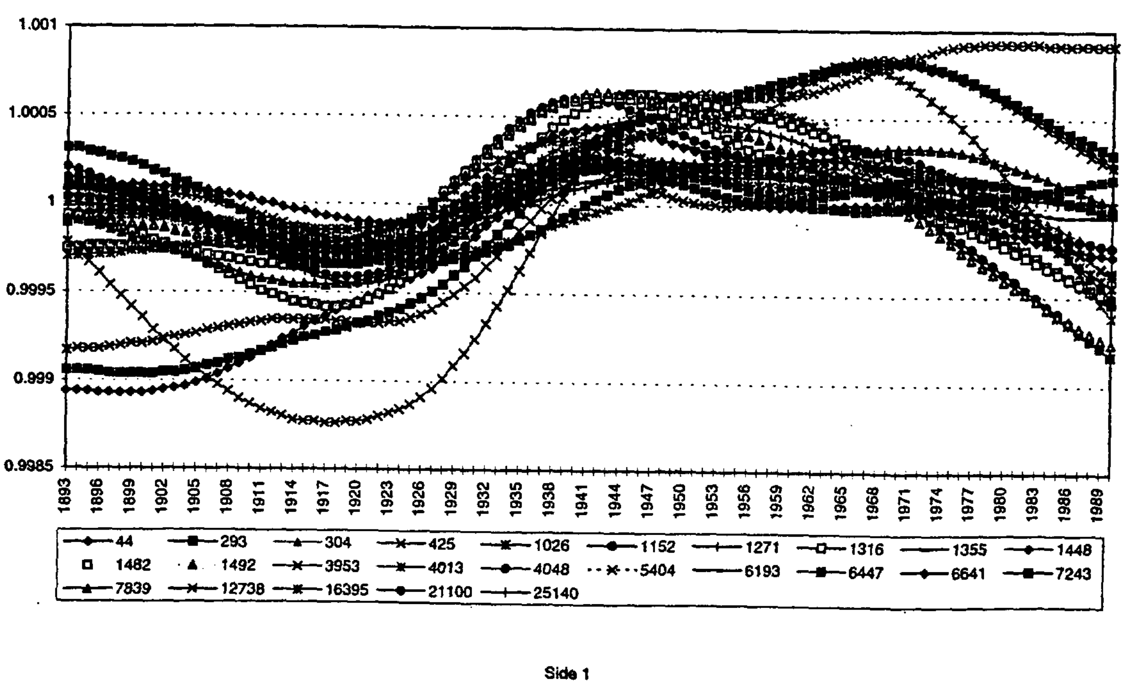

Figure 3.5 Filtered pressure series 1893-1990.

The British series have much of the same patterns as the Irish, both not that pronounced. There are significant trends in these series, also around 1937.

The Icelandic series 4013 Stykkisholmur has the same general characteristics as the British series. It has a little different behaviour in the last years, with a decreasing trend. The statistics shows no clear trends other than a significant decrease since the beginning of the sixties. The series of 4048 Vestmannaeyear has no significant trends, though the patterns are similar to Stykkisholmur.

All the Norwegian series have the same patterns, with the most significant trends in the western parts. There is a negative trend the first 35 years of the period. Then there is a positive trend until around 1945, significant at some stations (Oslo, Ferder, Bergen). All series have a significant negative trend since the 1930'ies with respect to the backward test statistics, except the Tromsø series, where the negative trend begins in the late fifties.

The series of Sweden can be split into two parts, eastern and western. The western series of Gothenburg have the same patterns as the Norwegian series, with a significant negative trend until 1928. In the eastern parts of Sweden and Finland there are no trends. The Danish series have no significant trends, except 6193 Hammerodde lighthouse, where a significant positive trend has been present since 1977.

The Belgian series of Uccle (6447) has a significant negative trend until 1936, and a positive trend afterwards.

4. EOF-ANALYSIS .

4.1 The method of empirical orthogonal functions (EOF).

EOF-analysis has been widely used for climatological and hydrological purposes for the last three decades (e.g. Gottschalk, 1985, Pandzic, 1988, Hanssen-Bauer et.al, 1996). The principle of the method is to decompose a number of correlated time series into a new set of uncorrelated functions. This decomposition can be expressed as:

$$X_i(t) = \sum_{j=1}^{m} h_{ij} \beta_j(t)$$

where $X_i(t)$ is the observed series, h_{ij} are the eigenvectors, or weights of the empirical orthogonal functions $\beta_j(t)$. i is the index of series, j is the index of components. m is the number of functions, equal to the number of input series.

The EOF-analysis results in two matrixes. One contains the orthogonal functions (amplitude functions) $\beta_j(t)$, which describes the variation of the components in time. The other matrix contains the eigenvectors(also called loadings or weight coefficients) h_{ij} of the eigenvalues. This matrix explains the spatial variation of the amplitude functions.

The total variance of the amplitude functions $\beta_j(t)$ contains the same variance as the total variance of the input series, but unlike the input series, the amplitude functions are uncorrelated. They can be considered as the EOF's in time, and they are ordered by their portion of the original variance, so that the function containing most of the total variance is ordered as function number one, the function with secondmost explanation of the total variance as number two and so on. If all the PCs are considered, the original series are restored.

One advantage with EOF-analysis, is that the amount of information is reduced. Most of the total variance is explained by a few EOFs. EOF-analysis is based on the same principle as principal component analysis (PCA), widely applied for spatial analysis of time series.

4.2 EOF-analysis of observed values.

Table 4.1 shows the portion of variance explained by the individual components at the series entered the EOF-analysis. Figure 4.1 show the time series of the first three eigenfunctions. Minimum value for EOF-1 is obtained in 1933. Maximum EOF-1 occurs in 1923. The observed pressure patterns of these years are shown in figure 4.2.

We observe a clear difference in the patterns of the two years. 1923 is characterized by cyclonic patterns. Strong westerlies over the British Isles and Scandinavia and a marked lowpressure over Island is present. The pattern of 1933, the year of minimum EOF-1, has generally a southwestern component. A high pressure ridge is present over Southern Norway. The pressure gradients are weak.

Interpretation of mean pressure fields like this is speculative, and should not be much emphasized.

Table 4.1 Portion of variance explained by the EOF's.

STNR	EOF-no. 1	2	3	4	5	6	7	8	(of 31)
44	0.75	0.01	0.17	0.01	0.00	0.02	0.01	0.00	
293	0.67	0.07	0.20	0.02	0.00	0.01	0.00	0.00	
304	0.58	0.16	0.17	0.01	0.04	0.02	0.00	0.00	
425	0.52	0.10	0.31	0.03	0.01	0.01	0.00	0.00	
1001	0.09	0.44	0.30	0.06	0.00	0.04	0.03	0.01	
1026	0.36	0.55	0.00	0.01	0.04	0.00	0.02	0.00	
1152	0.54	0.42	0.00	0.00	0.01	0.00	0.00	0.00	
1271	0.86	0.11	0.00	0.00	0.01	0.00	0.00	0.00	
1316	0.95	0.00	0.01	0.00	0.01	0.02	0.00	0.00	
1355	0.96	0.01	0.00	0.00	0.00	0.01	0.00	0.00	
1403	0.93	0.02	0.01	0.01	0.01	0.01	0.00	0.00	
1448	0.95	0.01	0.00	0.01	0.00	0.01	0.01	0.00	
1482	0.94	0.01	0.02	0.01	0.00	0.00	0.00	0.00	
1492	0.90	0.04	0.02	0.01	0.01	0.00	0.00	0.01	
3953	0.12	0.46	0.14	0.23	0.01	0.00	0.00	0.02	
4013	0.07	0.20	0.64	0.03	0.02	0.02	0.00	0.00	
4048	0.13	0.13	0.66	0.02	0.00	0.01	0.04	0.00	
5404	0.44	0.44	0.06	0.04	0.00	0.01	0.00	0.01	
6193	0.65	0.19	0.08	0.02	0.01	0.00	0.01	0.00	
6260	0.24	0.72	0.00	0.00	0.01	0.02	0.00	0.00	
6280	0.35	0.60	0.00	0.00	0.01	0.01	0.00	0.00	
6380	0.14	0.78	0.00	0.00	0.03	0.03	0.00	0.00	
6447	0.15	0.77	0.00	0.01	0.01	0.04	0.00	0.00	
6641	0.75	0.05	0.11	0.02	0.03	0.00	0.00	0.01	
7243	0.89	0.02	0.04	0.01	0.01	0.00	0.00	0.00	
7501	0.34	0.55	0.03	0.03	0.02	0.01	0.00	0.01	
7839	0.80	0.00	0.11	0.00	0.07	0.00	0.00	0.00	
12738	0.71	0.22	0.02	0.01	0.01	0.00	0.00	0.00	
16395	0.40	0.50	0.04	0.03	0.00	0.01	0.00	0.01	
21100	0.80	0.15	0.00	0.02	0.00	0.00	0.00	0.01	
25140	0.68	0.28	0.01	0.01	0.00	0.00	0.00	0.01	
Mean	**0.57**	**0.83**	**0.93**	**0.95**	**0.96**	**0.97**	**0.98**	**0.98**	

The eigenvectors show the spatial variability of the influence of the amplitude functions. If we interpret the amplitudefunctions as signatures of pressure patterns, the eigenvectors will show the different influence of these patterns in different areas. Figure 4.3a shows the spatial distribution of the first eigenvector, and figure 4.3b the portion of variance explained by this coefficient.

We see that the patterns of the Norwegian series are covered by the first component. This is not surprising, since this area is represented by a denser station cover than other parts of the study area. It is normal that the central area of an EOF-analysis has a high portion of variance explained by the first EOF, due to high spatial covariation.

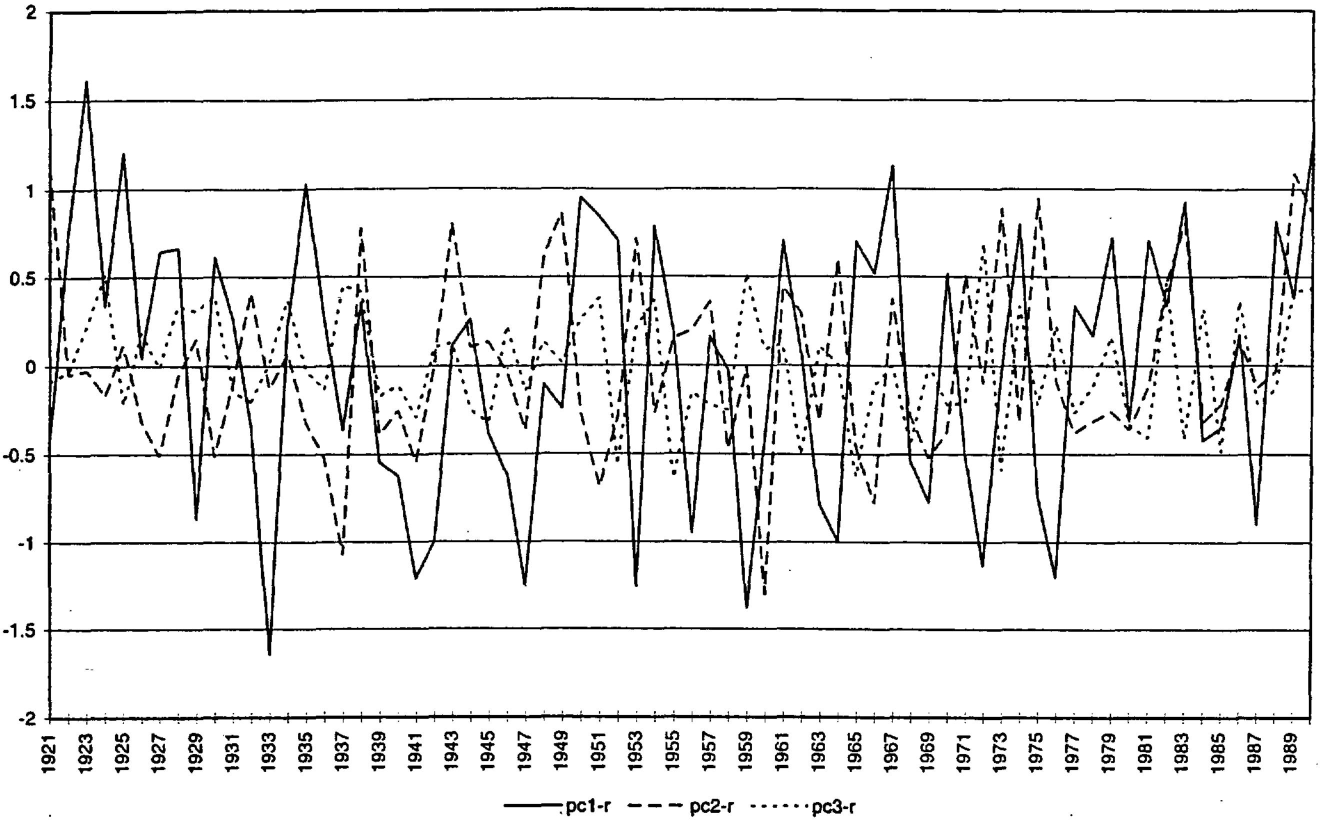

Figure 4.1 The timeseries of the EOF's.

From figure 4.3b it is seen that EOF-1 explains more than 90% of the pressure in southern Norway. The pressure variarions at Iceland and Jan Mayen are not explained by the first function at all (below 10%), and the contribution to Ireland is also low (12%).

Figure 4.4a shows the eigenvector of the second component. This component has positive loadings in the southern parts and negative loadings in the northern parts. In midlatitudes the coefficient is around zero, and therefore of low significance. This is confirmed by figure 4.4b showing the degree of variance explained by the second function. In the area explained by the first EOF, the second EOF explains very little, for most stations in southern Norway less than 5%. The component explains most (~75%) of the Belgian and Dutch series. It also gives a significant contribution to the Irish and northeastern series.

The third EOF explains the variability of the northwestern parts of the area (figure 4.5a), and can be called the Icelandic component. It explains more than 60% of the variations in the Icelandic series (figure 4.5b).

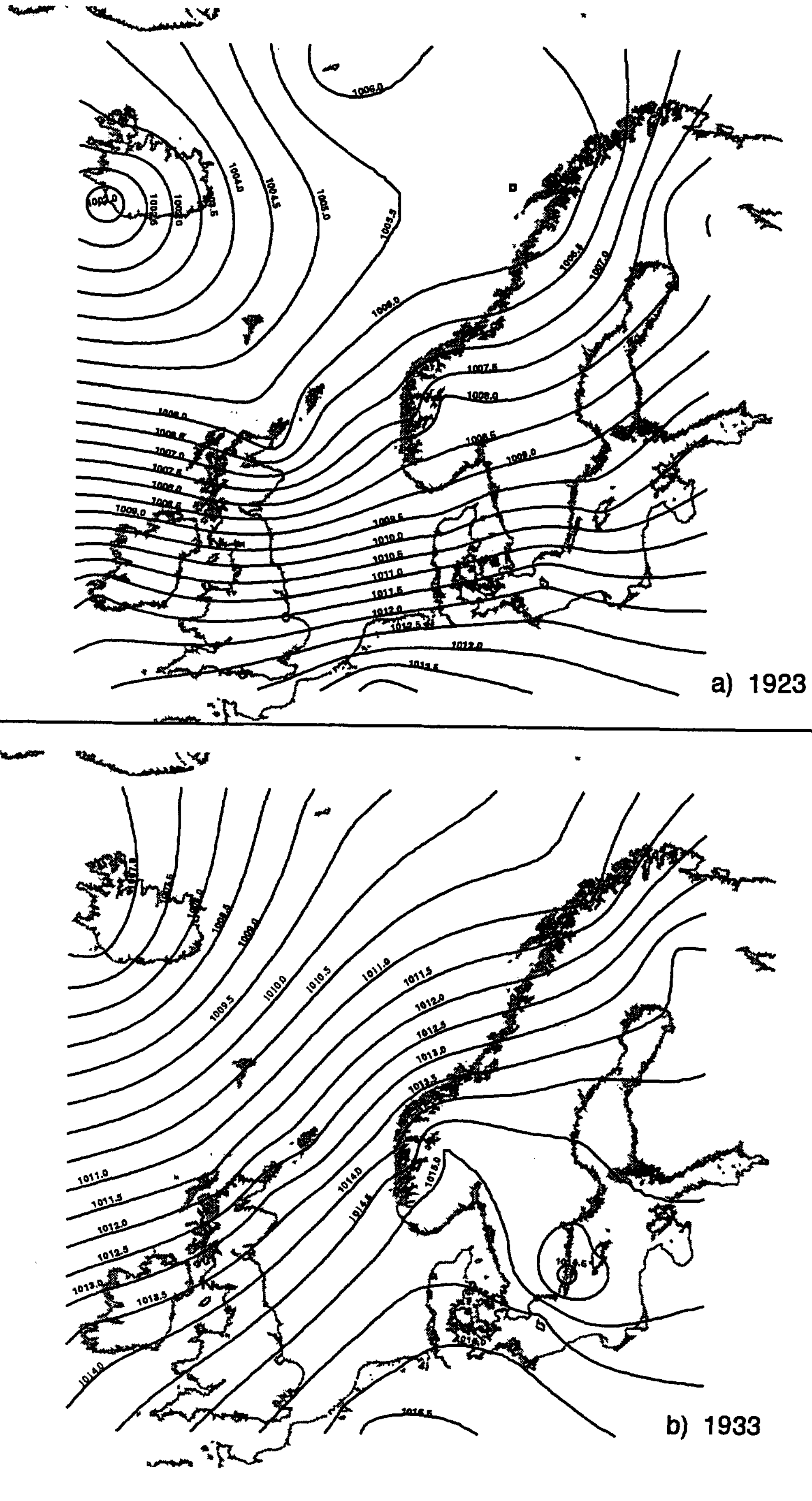

Figure 4.2 The mean annual observed pressure patterns of 1923(a) and 1933(b).

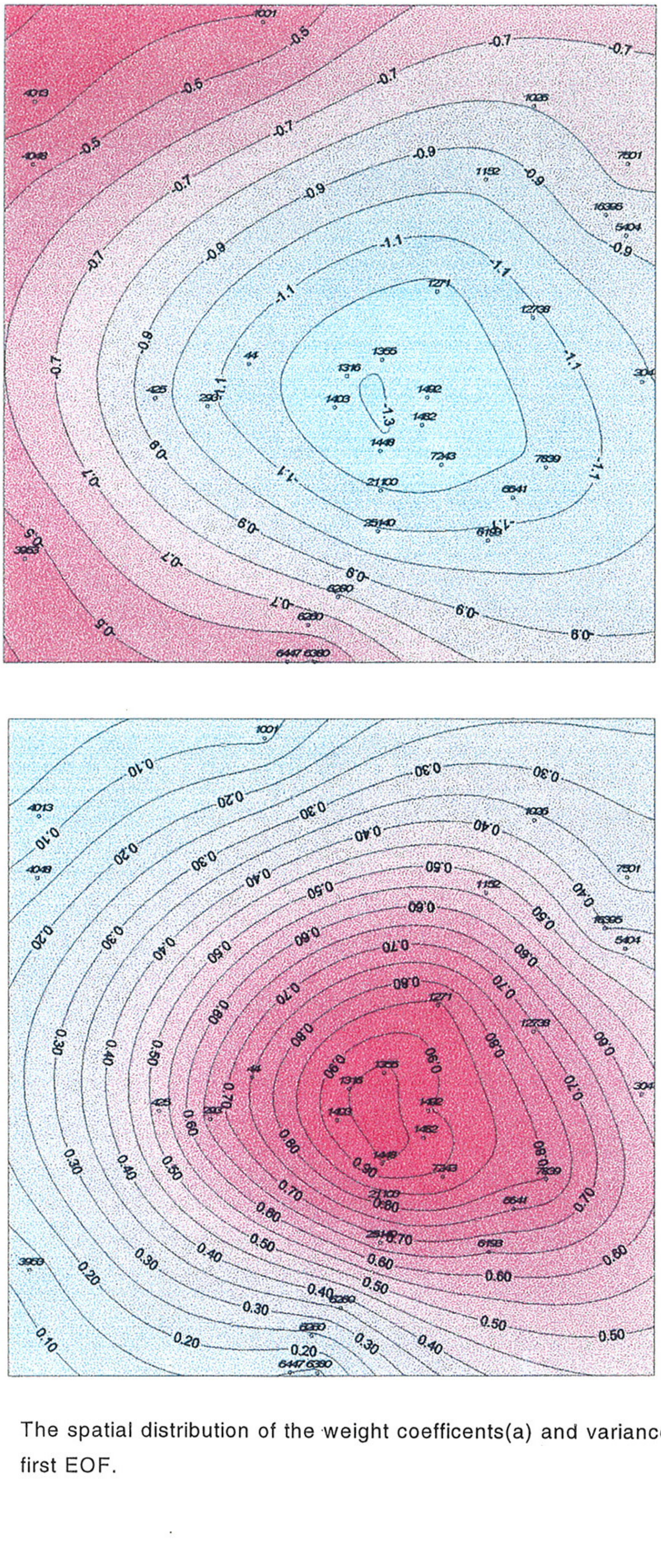

a)

b)

Figure 4.3 The spatial distribution of the weight coefficents(a) and variance contribution(b) by the first EOF.

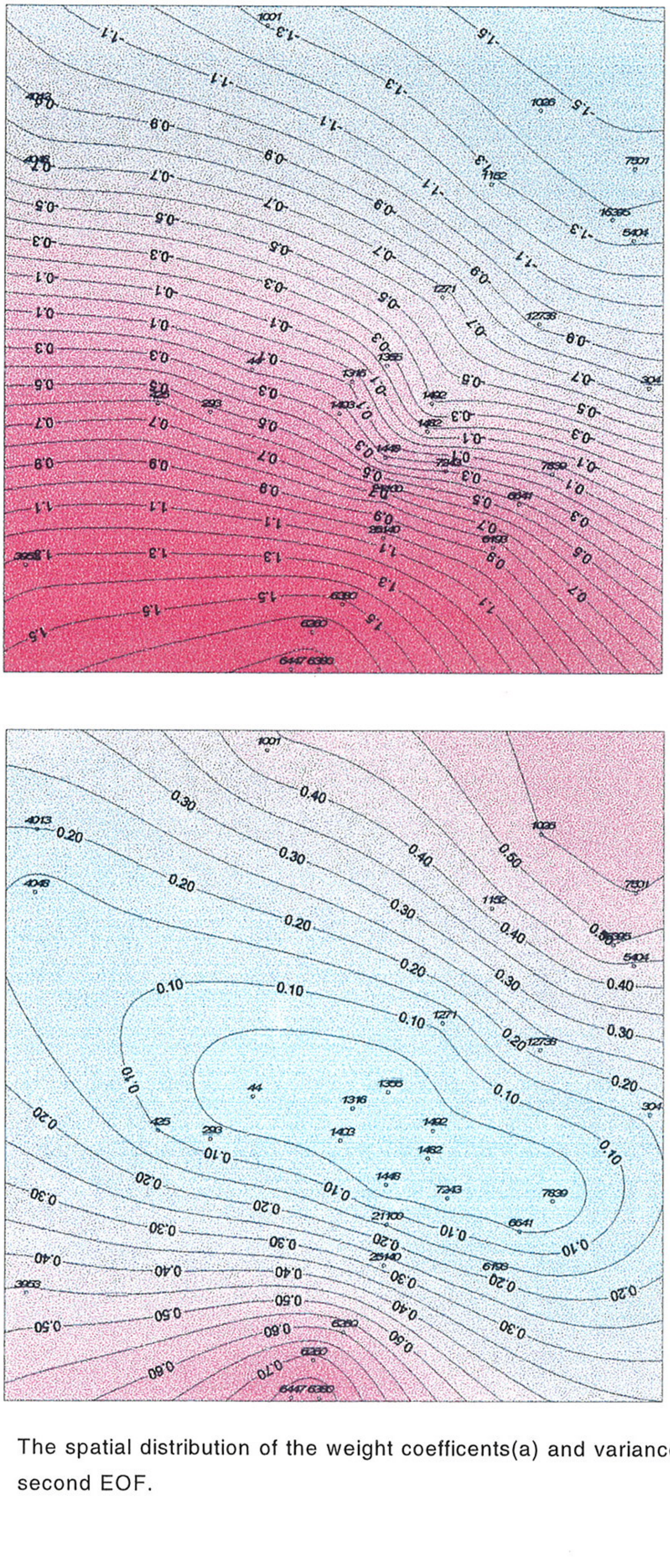

a)

b)

Figure 4.4 The spatial distribution of the weight coefficents(a) and variance contribution(b) by the second EOF.

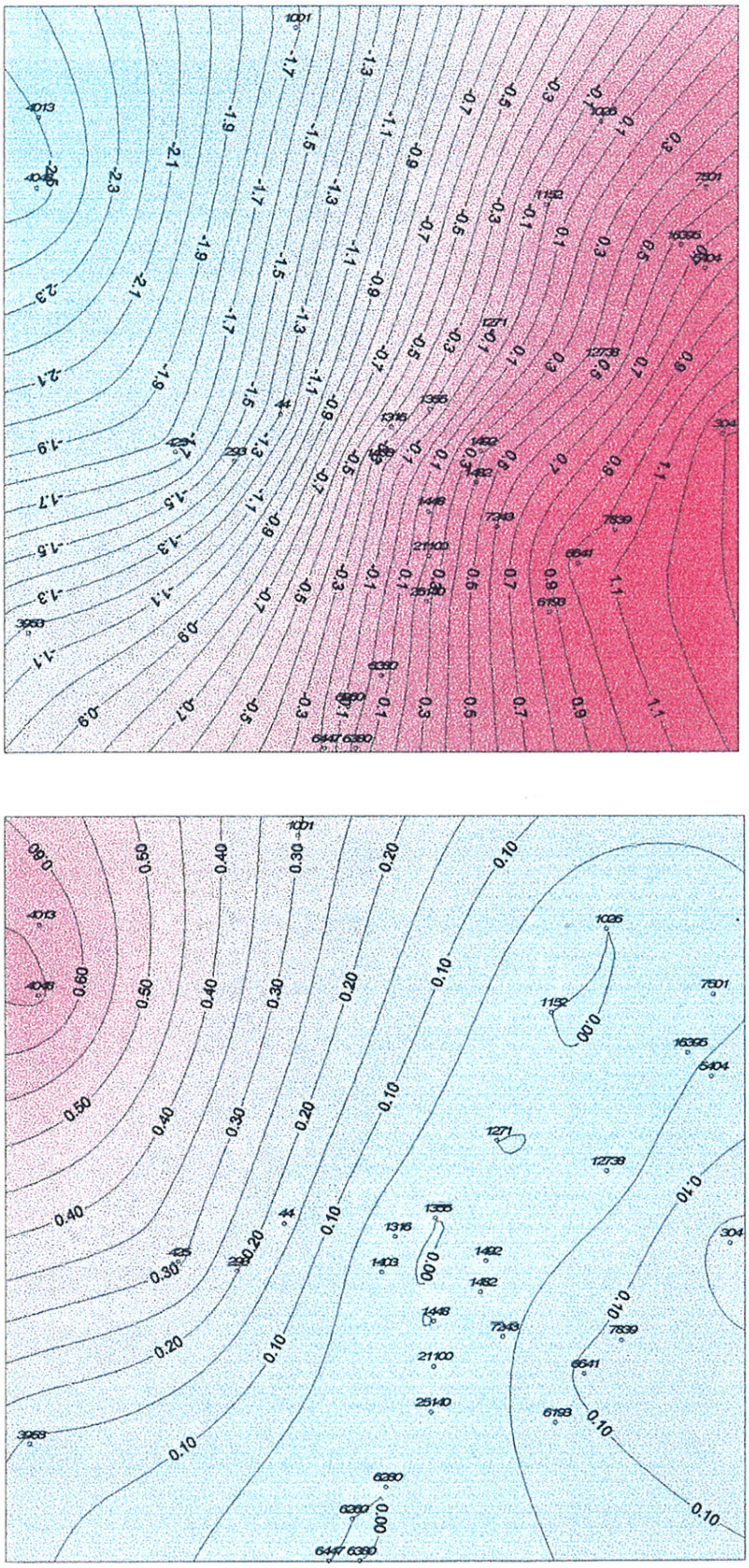

a)

b)

Figure 4.5 The spatial distribution of the weight coefficents(a) and variance contribution(b) by the third EOF.

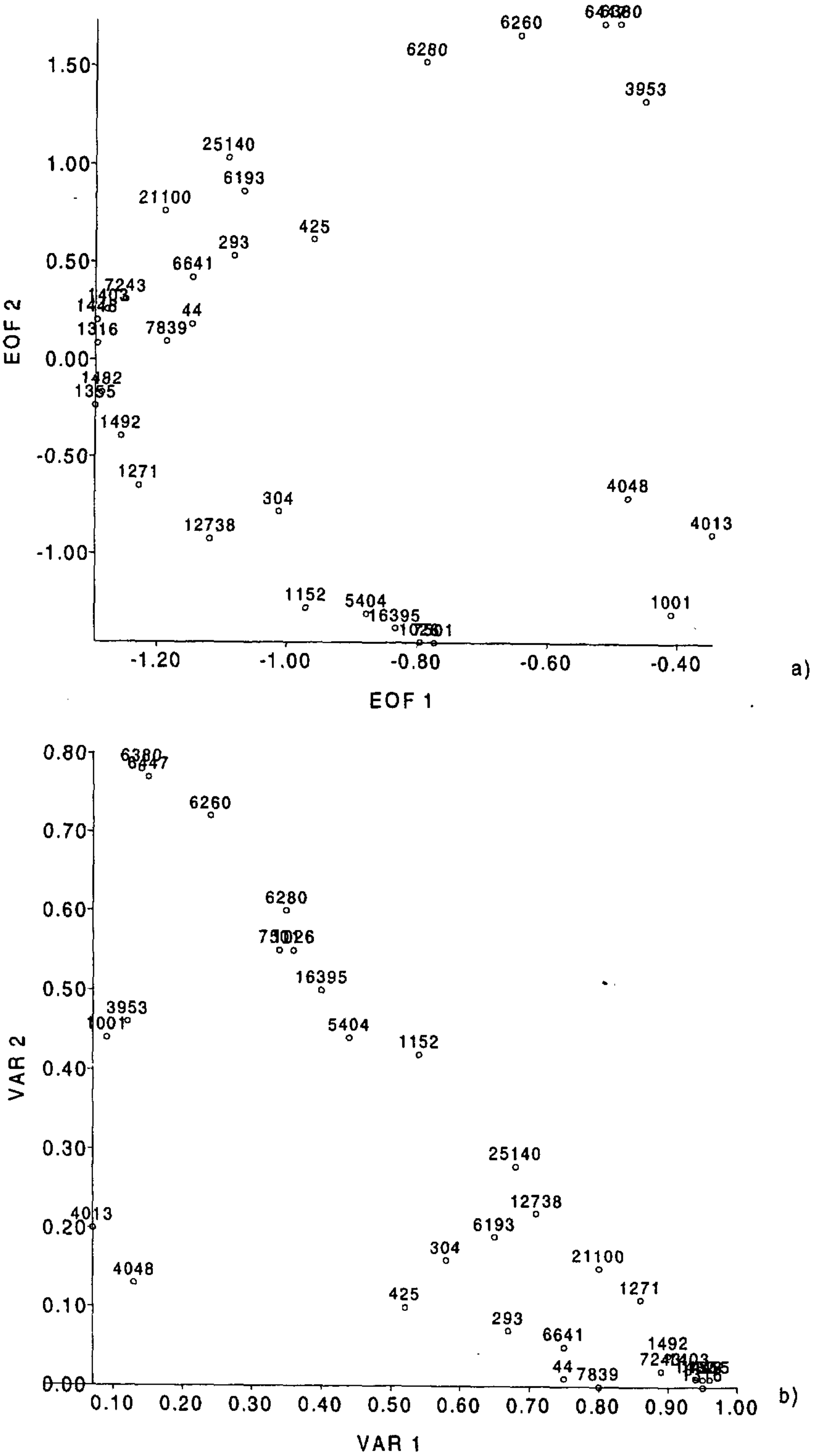

Figure 4.6 Scatter of the: a) loadings, b) variance contribution of the first and second EOF.

The series of Valentia, 03953, has a 24% explanation by the fourth series, the only series explained by more than 6% of this component. So the special pattern of this series is also recognized by the EOF-analysis.

Regionalisation

As pointed out above, the eigenvectors describe the spatial variation of the EOF's. They can therefore be used for regionalization with respect to the EOF's. Both the loadings and the proportion of variance can be used.

Figure 4.6a shows the scatter of the loadings of EOF-1 and EOF-2. The Scandinavian series is clustered around the minimum of EOF-1 axis. This means that these series get an important contribution from this component.

Figure 4.5b shows the same scatter, but for the variance. The scatter shows an almost linear relation between the two components. A large contribution from the first component implies a low contribution from the second, and vice versa.

The same procedure can be used for other combinations of eigenvectors (1-3, 2-3).

4.3 EOF-analysis of filtered values.

EOF-analysis was also performed on series smoothed by a Gauss-filter (filter length 9σ, approx. 30 years).

The same general tendencies as for annual values were found when performing an EOF-analysis on filtered values. The amplitude functions of the smoothed series have larger amplitude than the series resulting from filtered amplitude functions of raw annual series.

The table of portion of variance is shown in table 4.2. Compared to the analysis of "raw" annual series, the total cumulative variance seems to be almost the same. Regionally there are some differences. All variance in the filtered series is explained by just four components.

In the filtered series, the first component (fig 4.7a) explains the upper right triangle of the study area. The second component (fig 4.7b) explains the Irish series (3953 Valentia Obs.), and the third (fig 4.7c) explains mostly the variations in Belgium and

Holland. The fourth component makes a contribution in the southern parts of Finland.

If the correlation coefficients between the amplitudefuctions and regional trend curves (fig 3.3) are studied, the values shown in table 4.2 are found.

The sign of the correlation coefficient is not directly clear, since the contribution of the EOF also depends on the sign of the weights. Table 4.3 show the signs of the weights in the different regions.

Table 4.2a: Correlation coefficients between regional trend curves and filtered amplitude functions based on "raw" annual values (also fig 4.11a):

	Group I	Group II	Group III	Group IV	Group V	Group VI	Group VII	GroupVIII
EOF1	-0.43	-0.76	-0.87	-0.89	-0.91	-0.95	-0.90	-0.26
EOF2	0.90	0.56	-0.33	-0.44	0.29	-0.22	0.36	0.53
EOF3	0.05	-0.33	-0.25	0.12	-0.00	-0.02	-0.05	0.80
EOF4	-0.00	0.06	0.27	0.04	-0.29	-0.22	0.24	0.11
EOF5	0.00	-0.01	0.00	0.01	0.01	-0.05	-0.04	0.00

Table 4.2b: Correlation coefficients between regional trend curves and amplitude functions based on filtered annual values (also fig 4.11b):

	Group I	**Group II**	**Group III**	**Group IV**	**Group V**	**Group VI**	**Group VII**	**Group VIII**
EOF1	-0.36	-0.69	-0.90	-0.93	-0.87	-0.97	-0.86	-0.27
EOF2	0.91	0.61	-0.28	-0.39	0.36	-0.15	0.40	0.51
EOF3	0.02	-0.35	-0.29	0.11	0.02	0.00	-0.11	0.77
EOF4	0.09	0.11	0.30	0.11	-0.20	-0.16	0.31	0.26
EOF5	0.10	0.10	0.06	0.09	0.16	0.07	0.07	0.06

Table 4.3: Sign of the weights.

	Group I	**Group II**	**Group III**	**Group IV**	**Group V**	**Group VI**	**Group VII**	**Group VIII**
EOF1	÷	÷	÷	÷	÷	÷	÷	÷
EOF2	+	+	÷	÷	+	÷	+	+
EOF3	+	÷	÷	+	÷	0	+	+
EOF4	0	+	+	±	÷	÷	±	+
EOF5	+	÷(W) +(E)	+(W) ÷(E)	+(W) ÷(E)	÷	÷(W)+(SE)	÷	÷(E) +(W)

The correlation coefficients are approximately the same, taking care of the same patterns. It is seen again that the first component explains the trends in most areas except group I and VIII. These groups are explained by the second and third EOF.

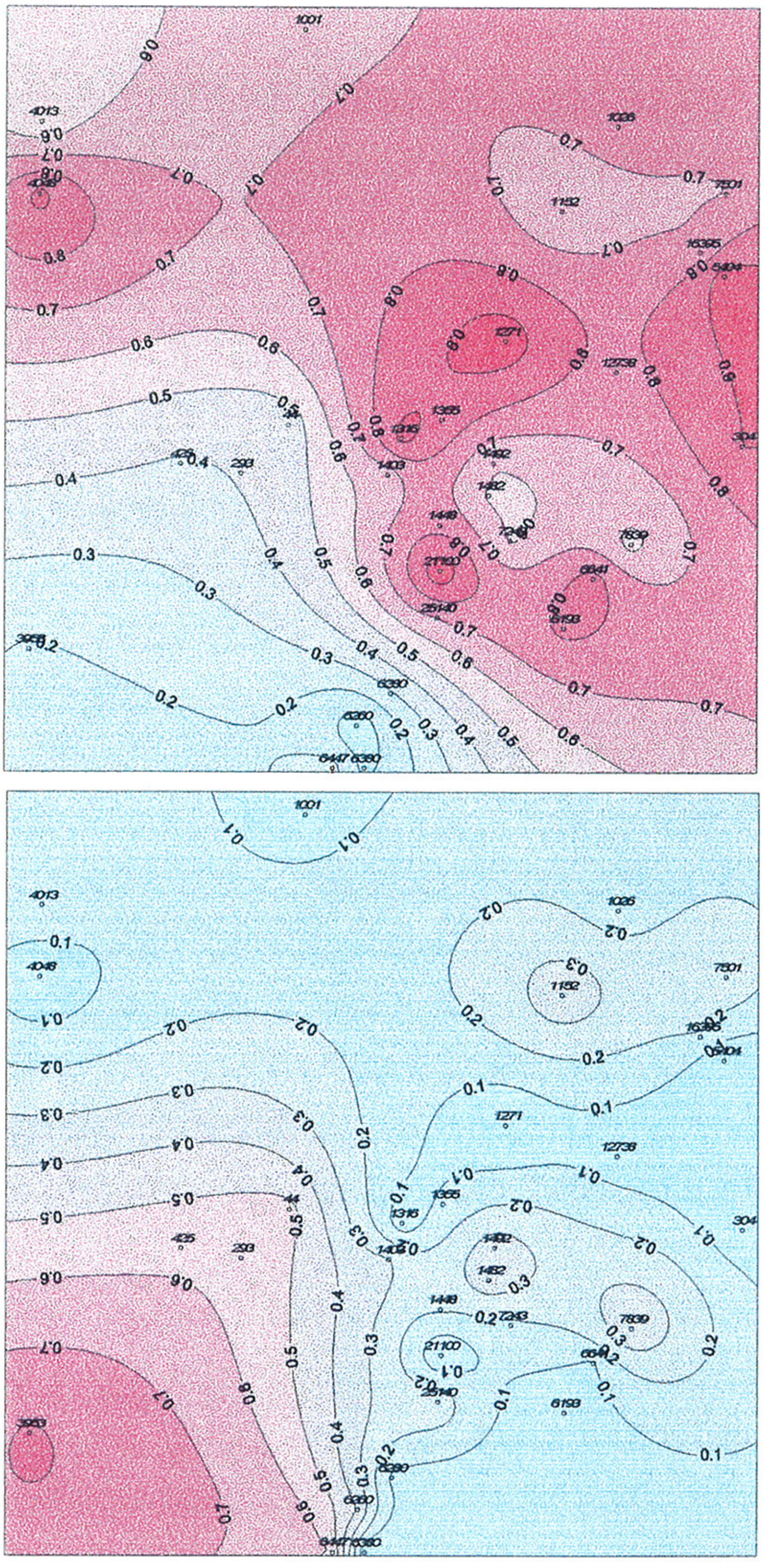

a)

b)

Figure 4.7 Spatial distribution of the variance contribution of the EOF's based on filtered series, EOF1 - (a), EOF2 - (b)

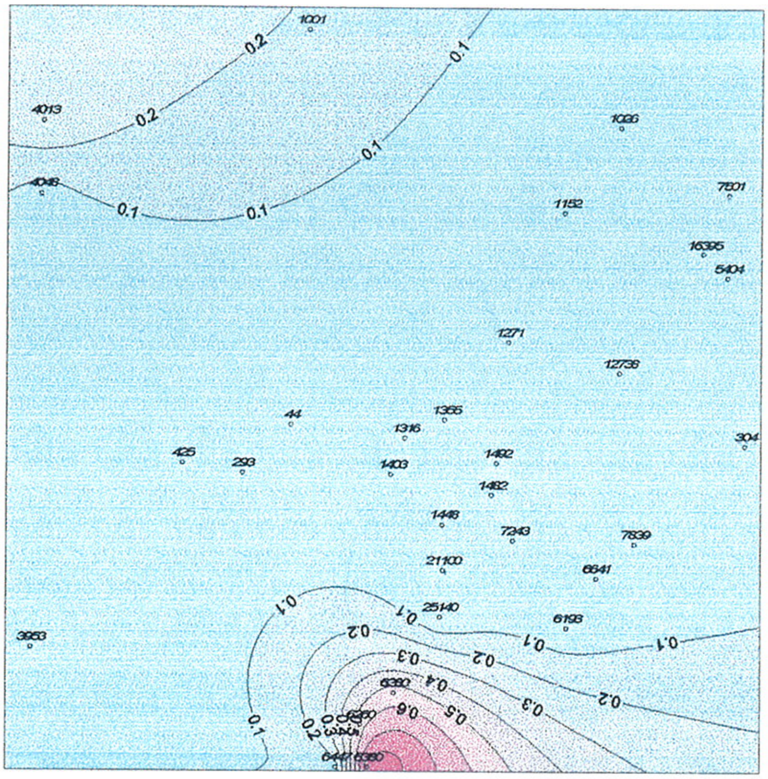

c)

Figure 4.7(Cont.) Spatial distribution of the variance contribution of the EOF's based on filtered series, EOF3 - (c).

The long time variations in the different regions can be explained by different components in different time periods. Therefore, it is not possible to connect one component to the variations in one specific region.

By looking at the distribution of the weight coefficients, it can be assumed that the first component is a mixture of zonal and meridional components. The variation of the central series in the dataset will dominate, mostly due to the dense station coverage in this area. The second EOF seems to account for meridional activity, and the third accounts for zonal winds.

There are problems connecting these results to clear circulation patterns, since the dataset is irregular in space. Some important features affecting circulation in the study area are not represented. Probably would series from the southeastern part of the study area bring new and important information about pressure variations, and give better understanding of these, especially in the area around the Baltic Sea.

5. VARIABILITY OF PRESSURE GRADIENTS

The variations of station pressure do not explain the variability of the large scale circulation. Pressure gradients may be used to describe the zonal and meridional winds. In this study the variability of four gradients is studied. The four profiles are shown in figure 5.1. Two of the profiles describe zonal winds (Z1 and Z2) and two meridional winds (M1 and M2). The profiles are selected because they represent the boundaries of the area studied.

Smoothed curves of the gradients are derived using the Gauss filter with filter length 9 standard deviations. The resulting curves for the period 1893-1990 are shown in figure 5.2. In the period 1893 to around 1945, the patterns of Z1 and M1 are similar. The patterns of Z2 and M2 also have the same tendencies in the same period. Z1 and M2 turn some years before the other two. In the last part of the period Z1 and Z2 have common parts, as well as M1 and M2.

The pressure gradient series was also tested by the Mann-Kendall test. The results (figure 5.3) of this test shows a significant negative trend from 1893 to around 1920 in Z1. After that a positive trend is present during the rest of the period.

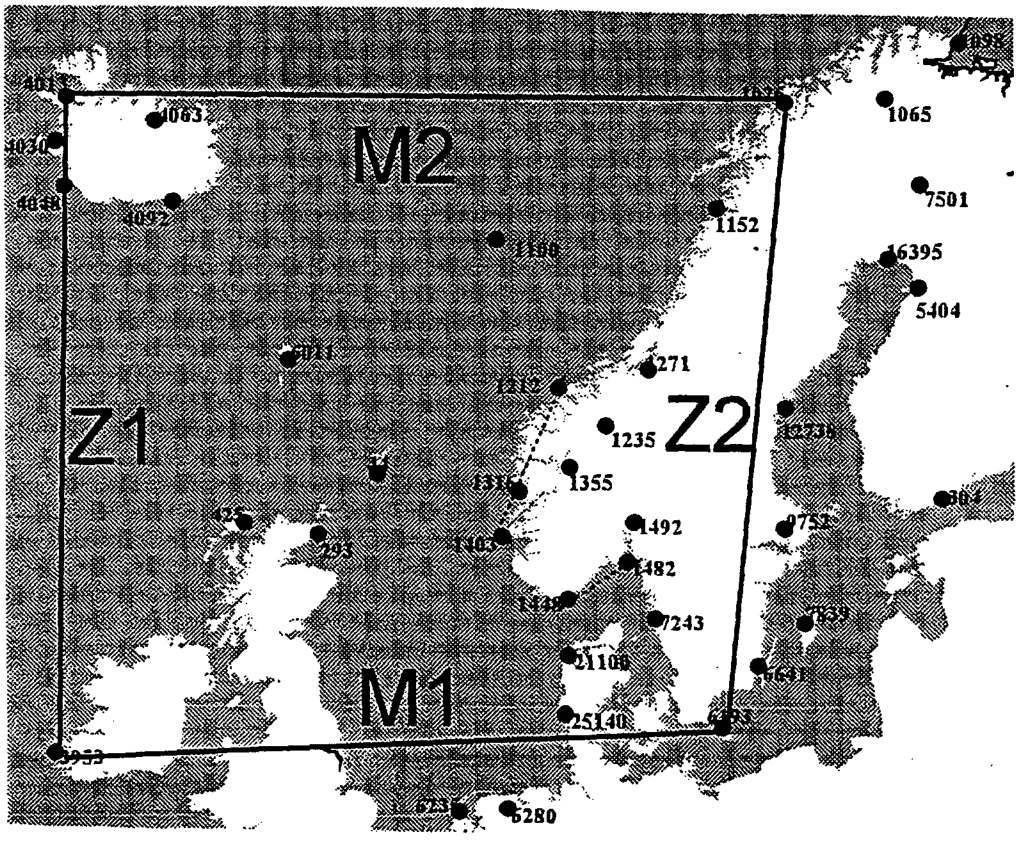

Figure 5.1 The gradients examined.

Profile Z2 has no significant trend with respect to forward statistics. The backward statistics show a significant trend the last years, though the period is a little bit short to make certain conclusions.

The meridional gradient M1 has a significant positive trend from 1930 and the rest of the period. In the first part of the period, a significant negative trend is present from 1893-1905. The backward test shows a postive significant trend between 1915 and 1935.

The M2 gradient has no significant trends, though the patterns are similar to the variations in the backward statistics of gradient M1 in the last part of the series. In the first part the statistics shows no systematic variations.

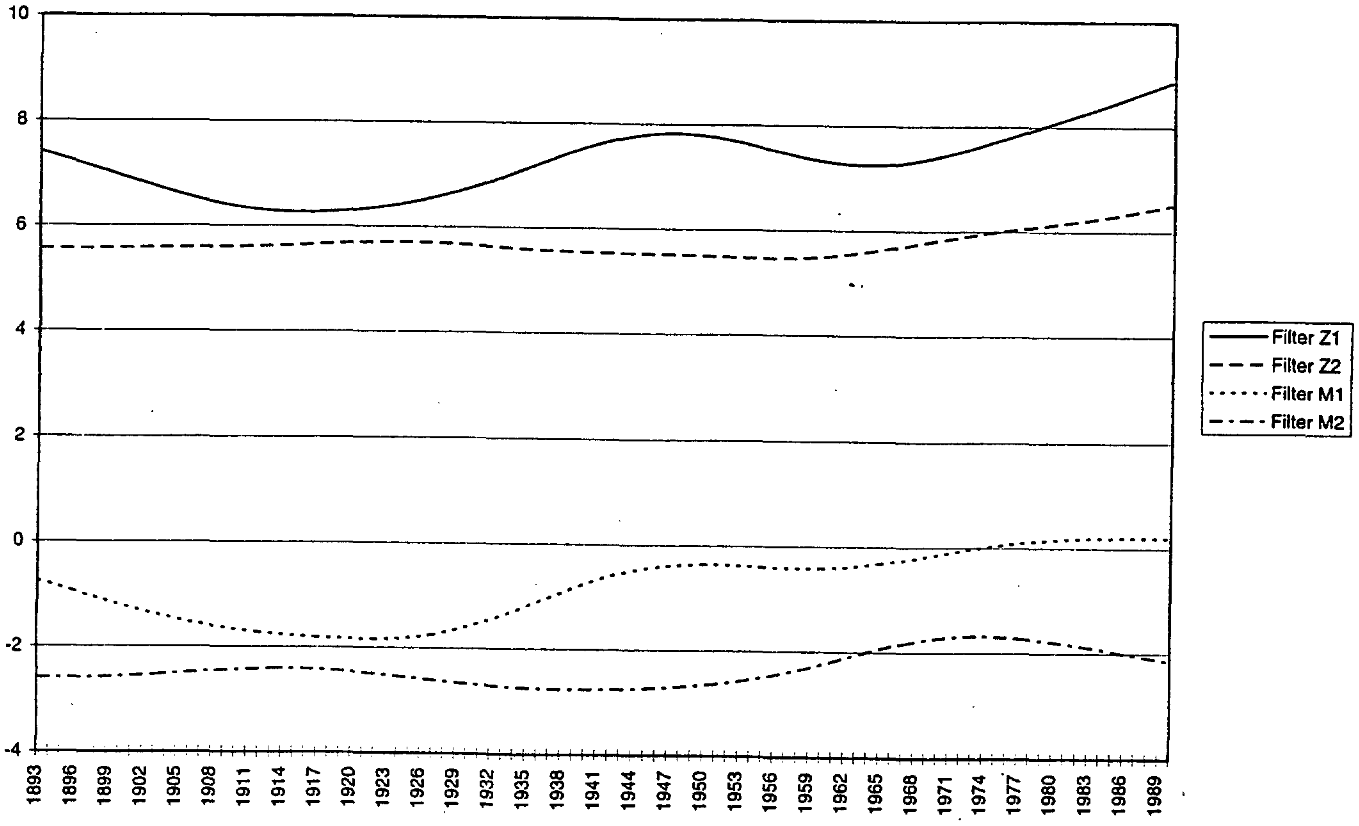

Figure 5.2 Trend curves of the gradients.

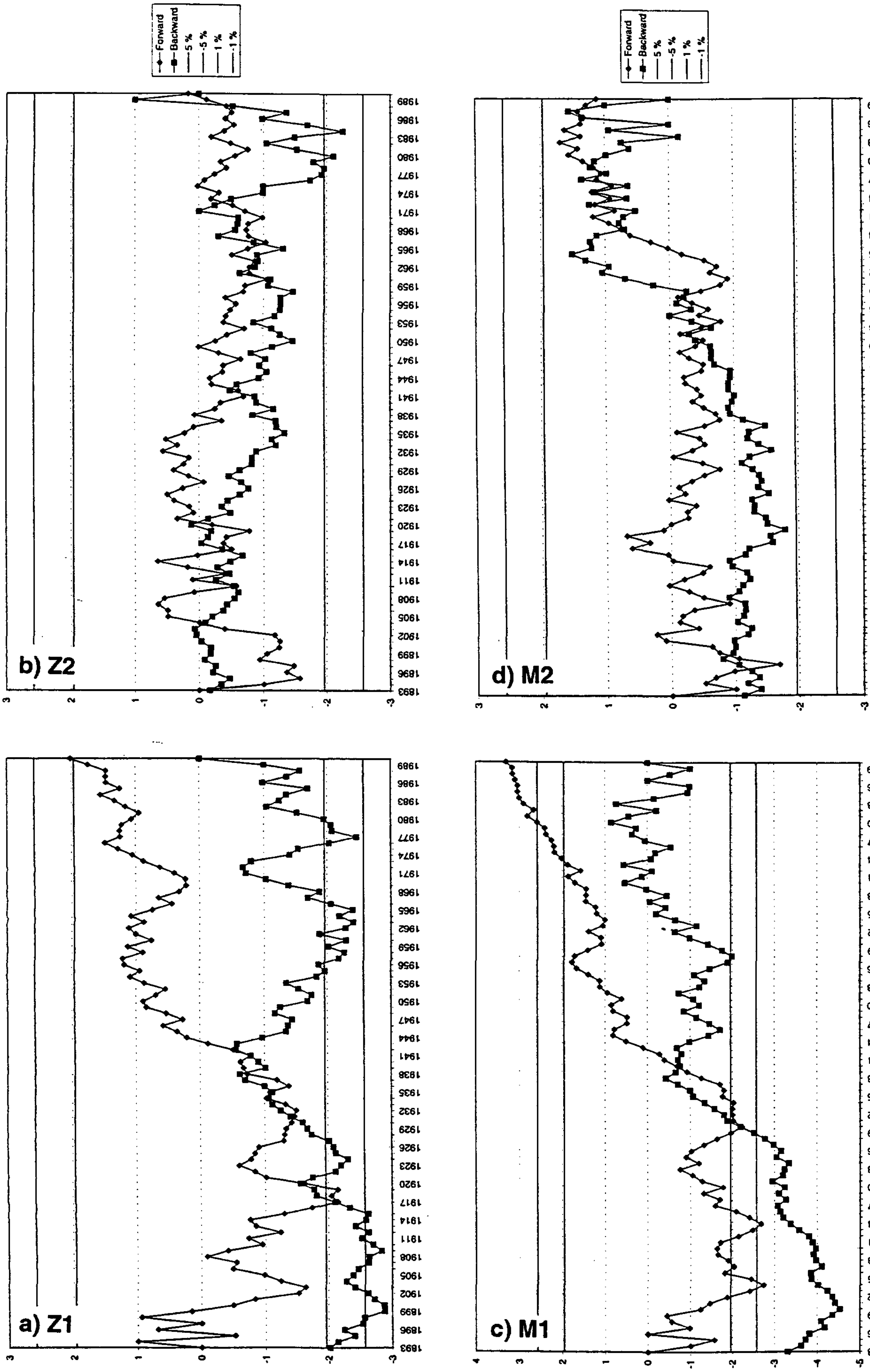

Figure 5.3 Mann-Kendall series of a) Z1, b) Z2, c) M1 and d) M2.

6. RELATION BETWEEN PRESSURE VARIABILITY AND OTHER CLIMATOLOGICAL ELEMENTS.

This little study of pressure variability reveals similarities with results from similar studies on other climatological elements.

Hanssen-Bauer et.al (1996) applied Principal Component Analysis on the NACD temperature series. The spatial patterns of the loadings are very similar. In the EOF's there are also similarities, though not so clear. The variances of the two processes are different, and this may lead to some different structures of the EOF's.
The relation between circulation and precipitation can be showed clearly by two examples from Norway. The first example, the precipitation series of Samnanger in western Norway, shows a very high correlation with the pressure gradient between 1403 Utsira and 1212 Ona. This profile shows almost directly the onshore component on the Norwegian west coast. Figure 6.1 shows the correlation between the pressure gradient and precipitation for each month and annual values for the period 1957-90. Figure 6.2 shows the March-series for the two variables. In this case a very strong relation between precipitation and zonal component is present.

The other example is a precipitation series at the south coast of Norway, Mestad near Kristiansand, figure 6.3. There are large variations in the relation between pressure gradient Oksøy(1448) -Ferder(1492) and precipitation in the period 1890 - 1990. In the period 1901-30 the correlation was 0.30 between the pressure gradient and precipitation. In the period 1931-60 the correlation was 0.10 and in the last period, 1961-90, 0.74. These variations may be explained by possible changes in circulation patterns.

7. CONCLUSIONS

This study of North-Atlantic pressures series showed variability in both time and space. Comparison of smoothed trend series made it possible to form eight groups related to these variations.

Analysing the series applying the method of empirical orthogonal functions (EOF) gives results supporting the comparison of trends results. EOF also shows similarities to the regional curves.

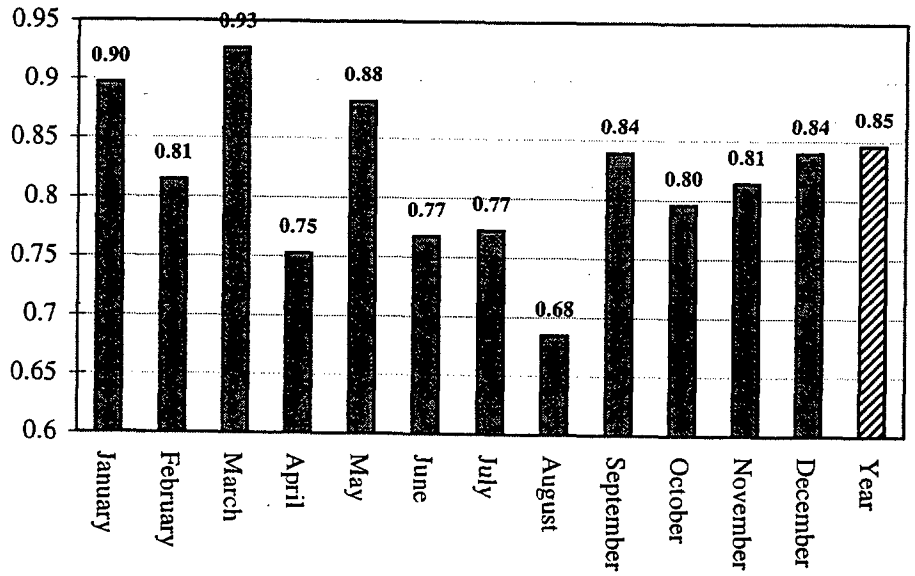

Figure 6.1 Correlations between the onshore presure gradient and precipitation at 50350 Samnanger.

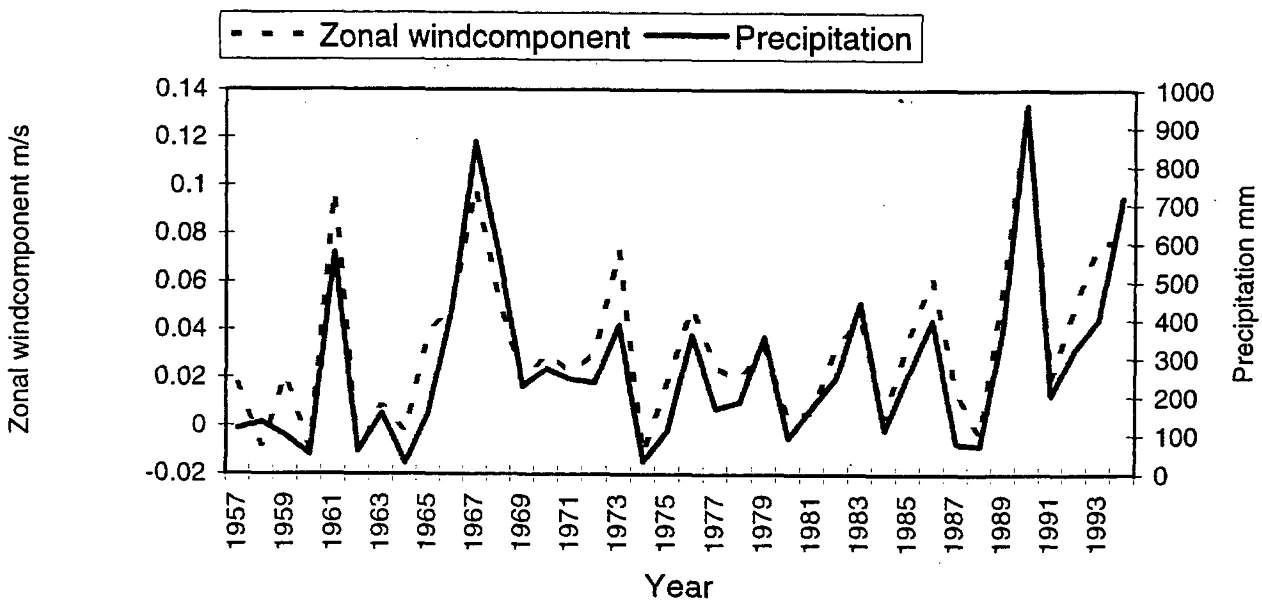

Figure 6.2 The series of on-shore pressure gradient and precipitation at 50350 Samnanger, march 1957-90.

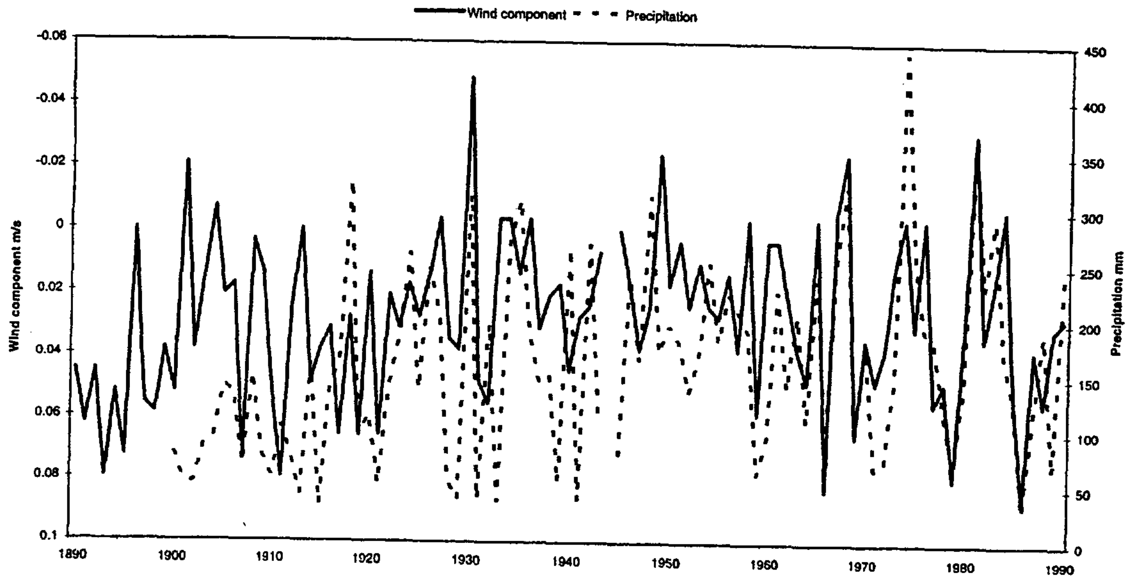

Figure 6.3 The series of onshore pressure gradient (meridional) and precipitation at 39220 Mestad, annual values.

Four pressure gradients were calculated to examine the variations in zonal and meriodonal components. The results indicates a change in the circulation patterns around 1945.

Mann-Kendall test shows significant trends in the pressure series as well as the pressure gradients. The trends are strongest in the western parts of the study area.

The variations and trends in the pressure series can also explain the breaks found when performing the homogeneity testing of the pressure series. In these tests noise around 1915-17 and in the thirties occurred, without situations causing homogeneity breaks described in inspection reports. In Norway none of these indicated breaks, caused by natural variability, was adjusted for.

The results of this introductory study on air pressure reveal interesting properties regarding the variations in circulation. These variations are influencing the variability of other climatological elements, like temperature and precipitation. Further research is needed to get a better understanding of the interdependencies of different climatological processes, and to understand the local effects of the circulation variations. Such research should include:

- Establishing circulation indexes for the North-Atlantic, and study the variations of these indexes over last 100 years.
- Using regular gridded data in the analysis, and compare the results to the results of the unevenly spatially distributed dataset used in this study.
- Find relations between circulation indexes and EOF's, and other climatological elements.

ACKNOWLEDGEMENTS.

The author gratefully acknowledges Eirik J. Førland for fruitful discussions during the investigations and critical comments upon this manuscript. Lars Andresen is acknowledged for his comments on the pressure fields in figure 4.2.

The study is partly founded through the NMR project REWARD and the European Commission project WASA.

REFERENCES:

Alexandersson,H., Eriksson,B. **(1989)**

Climate fluctuations in Sweden 1860-1987, *SMHI Reports, Meteorology and Climatology.*

Frich,P., Alexandersson,H., Ashcroft,J., Dahlström,B., Demareé,G., Drebs,A., van Engelen,A., Førland,E., Hanssen-Bauer,I., Heino,R.,Jónson,T., Jonasson,K., Keegan,L., Nordli,P.Ø., Schmith,T.Steffensen,P., Tuomenvirta,H. and Tveito,O.E. **(1996)**

North Atlantic Climatological Dataset (NACD), Final Report, *DMI Scientific Report 96-1, Danish Meteorological Institute, Copenhagen, Denmark*

Førland,E., van Engelen,A., Hanssen-Bauer,I., Heino,R., Ashcroft,J., Dahlström,B., Demareé,G., Frich,P., Jónsson,T., Mietus,M., Müller-Westermeier,G., Pálsdottir,T., Tuomenvirta,H.,Vedin,H. **(1996)**

Changes in "normal preciptation in the north Atlantic region, *DNMI Klima 7/96.*

Gottschalk,L. **(1985)**

Hydrological regionalization of Sweden, *Hydrol.Sci.J., 30,1,65-83.*

Hanssen-Bauer,I., Førland,E. and Nordli,P.Ø. **(1996)**

Principal component analysis of the NACD temperaure series, *DNMI Klima 1/96.*

Hanssen-Bauer,I., Førland,E., Tveito,O.E. and Nordli,P.Ø. **(1996b)**

Regional precipitation trends - Comparison of two methods, *Submitted to Nordic Hydrology*

Pandzic,K. **(1988)**

Principal component analysis of precipitation in the Adriatic-Pennonian area of Yugoslavia, *J.Climatol,8,357-370.*

APPENDIX A

Trend-Kendall series for the NACD-pressure series 1893-1990.

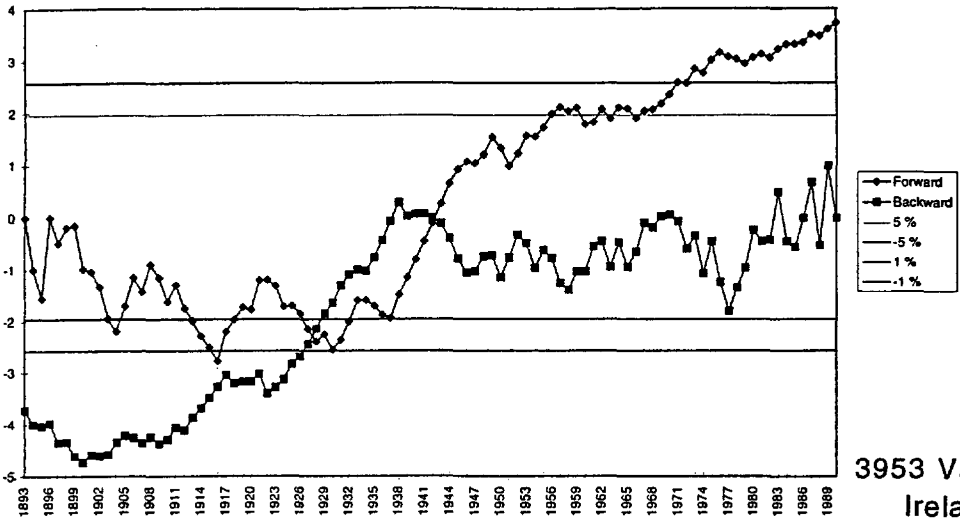

3953 Valentia Obs.
Ireland, Group I

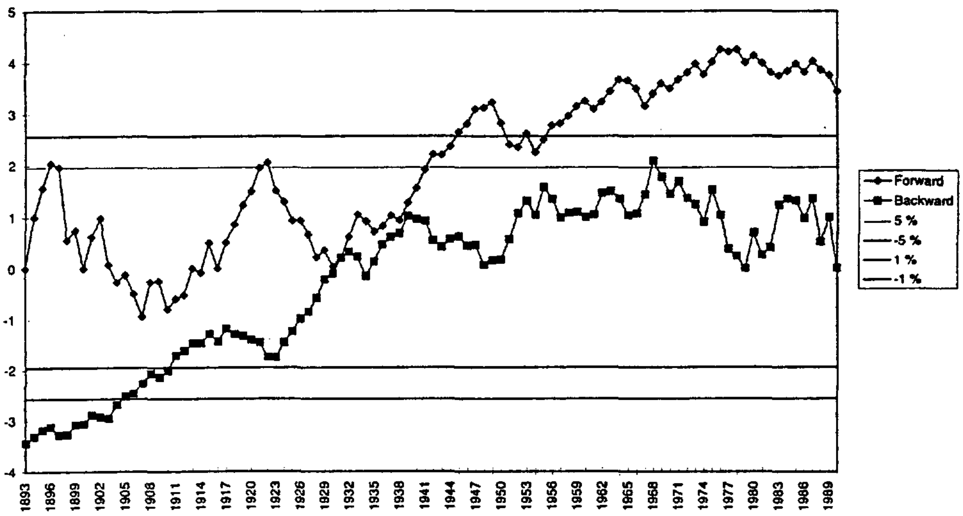

44 Lerwick
United Kingdom, Group II

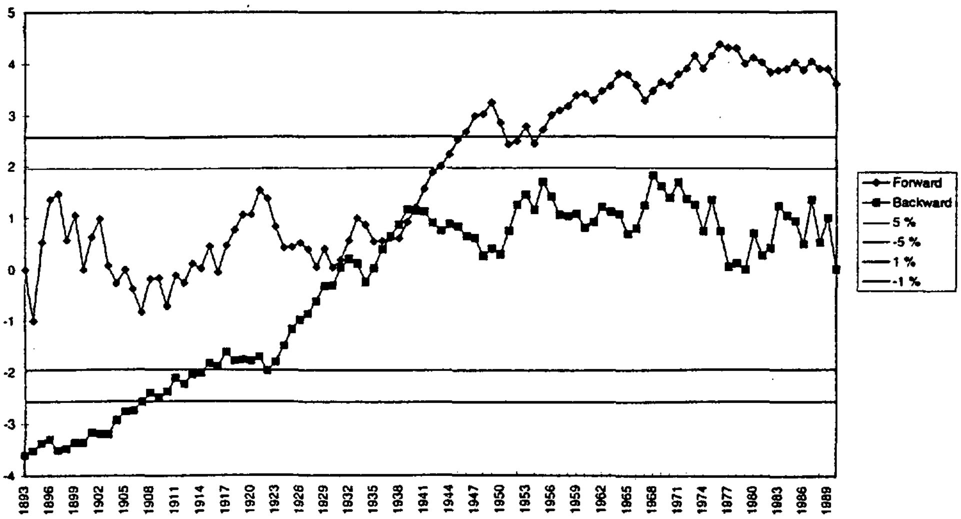

293 Wick
United Kingdom, Group II

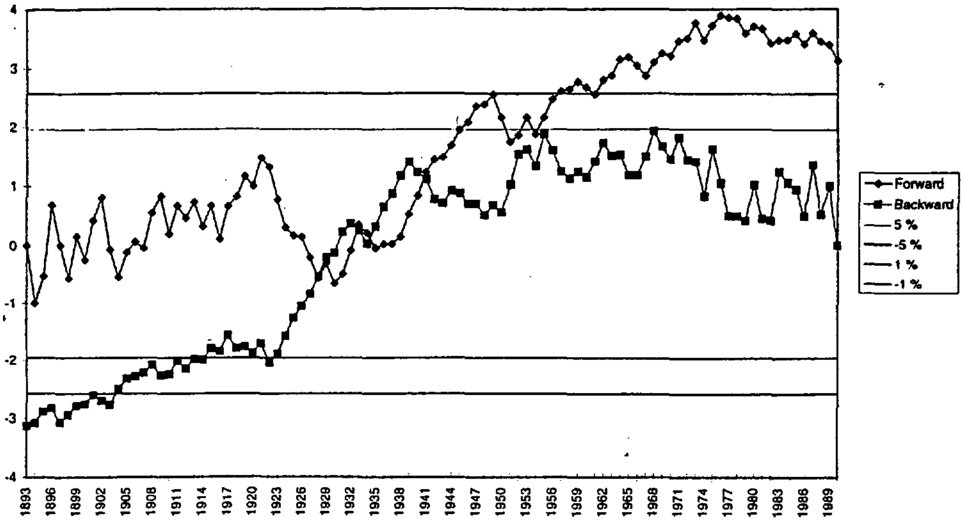

425 Stornoway
United Kingdom, Group II

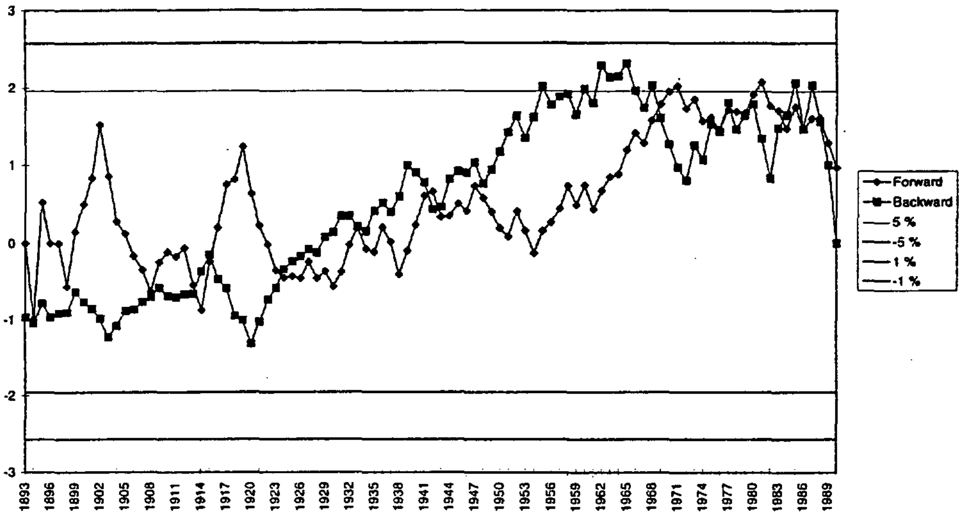

4013 Stykkisholmur
Iceland, Group II

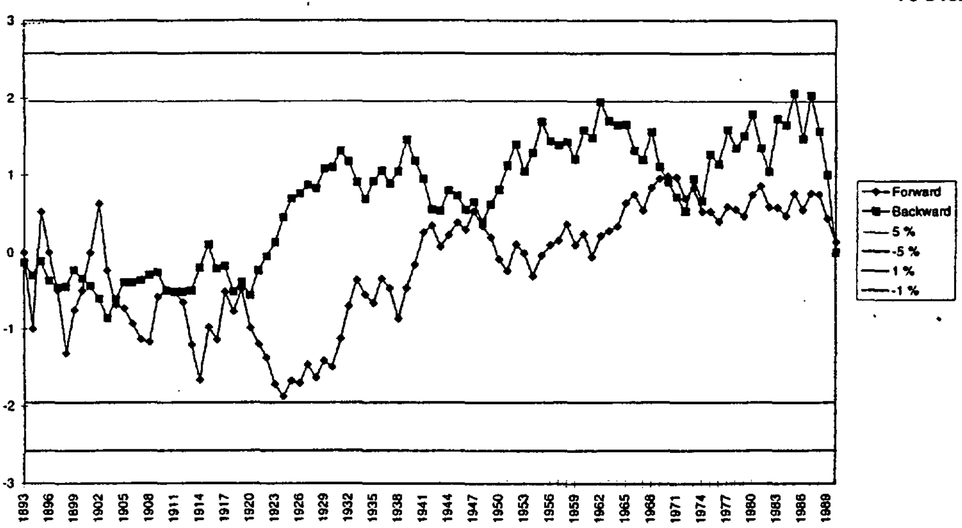

4048 Vestmanneyjar
Iceland, Group II

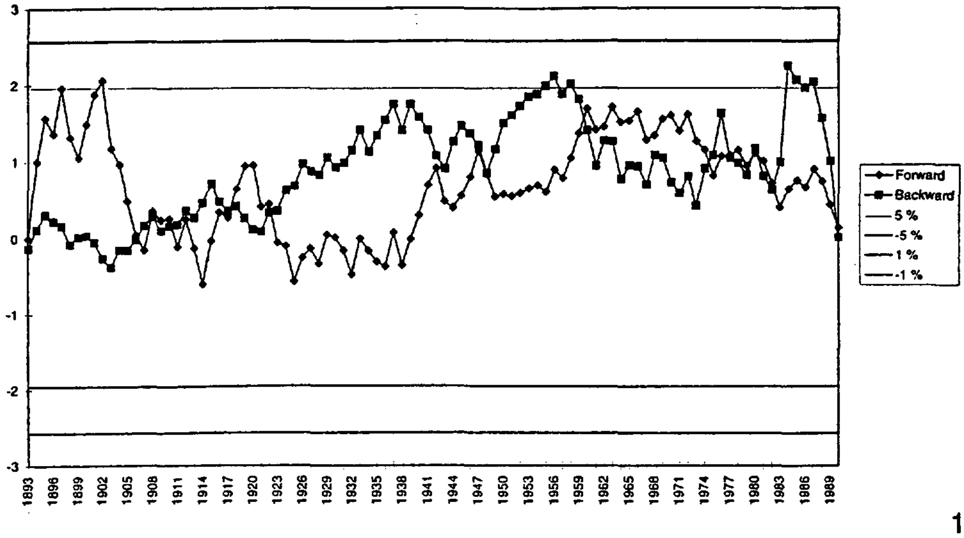

1026 Tromsø
Norway, Group III

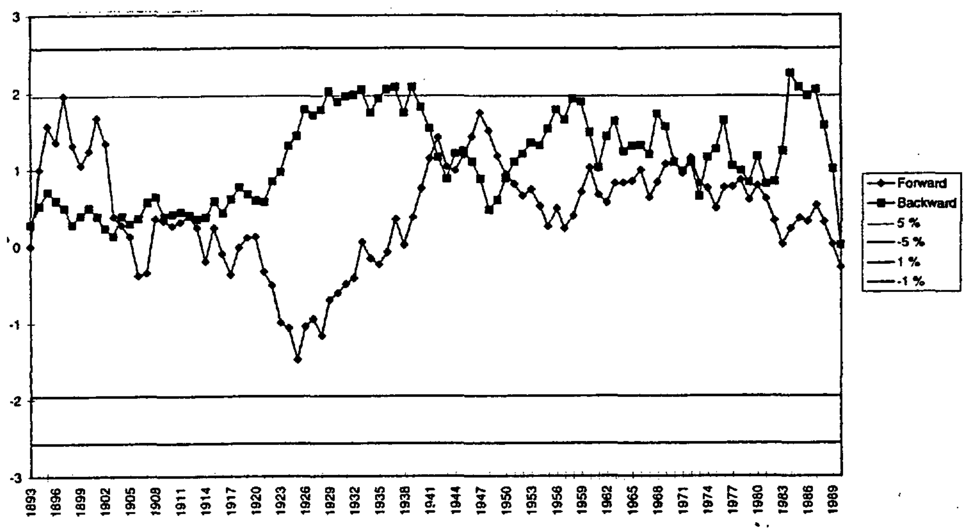

1152 Bodø
Norway, Group IV

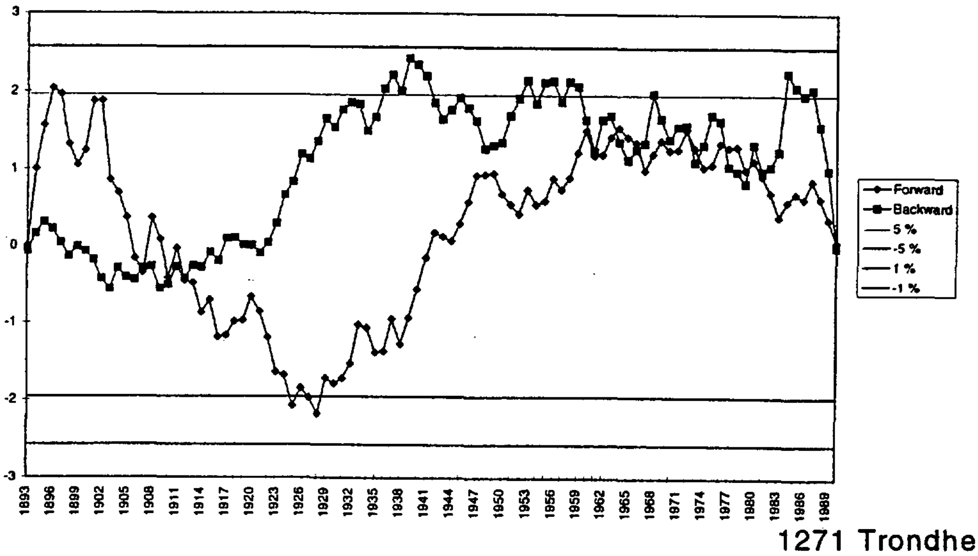

1271 Trondheim-Værnes
Norway, Group IV

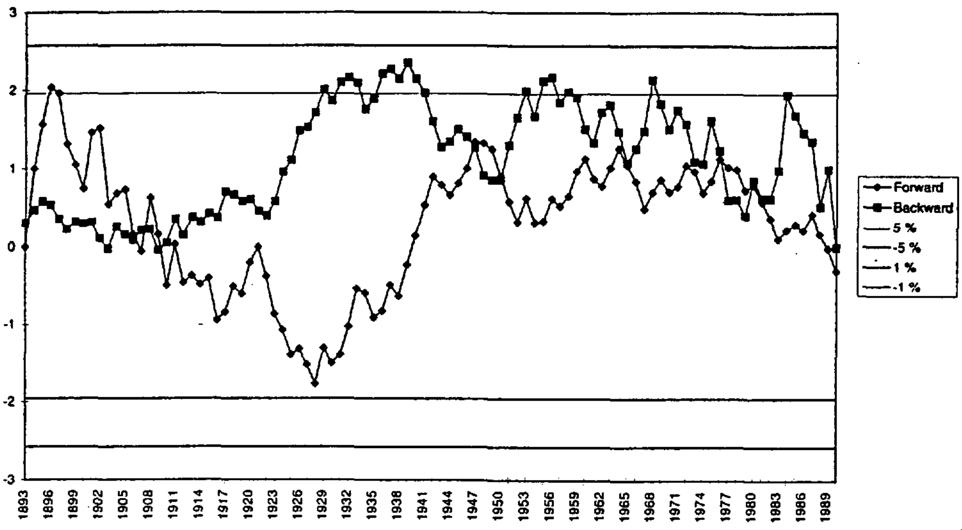

1355 Lærdal
Norway, Group IV

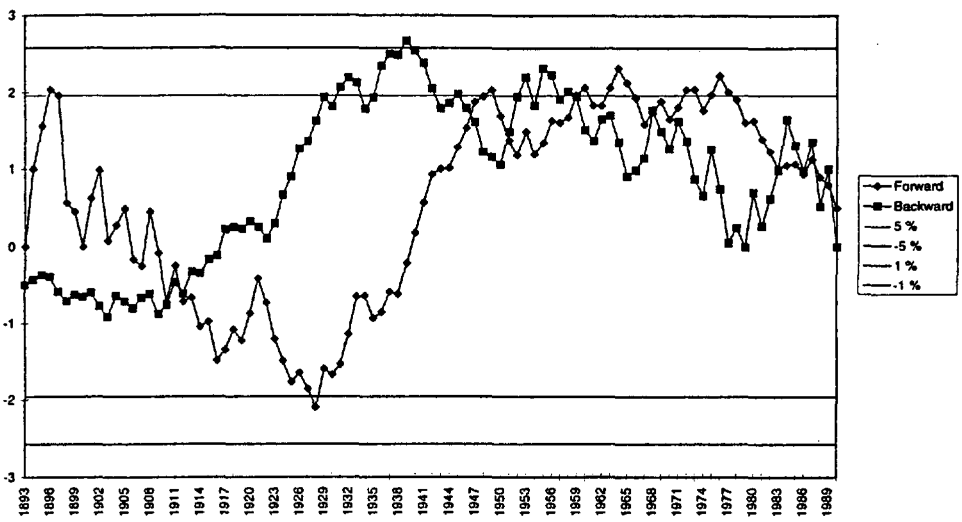

1316 Bergen-Florida
Norway, Group IV

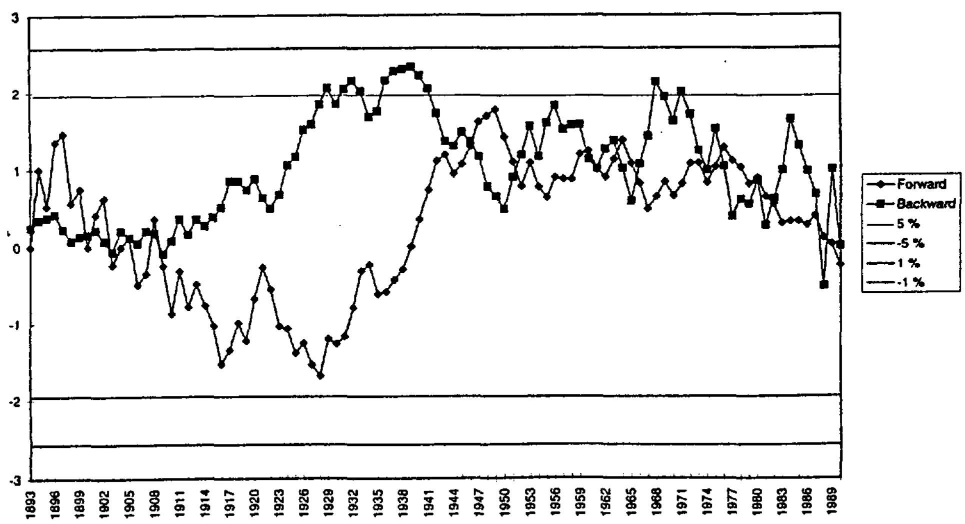

1448 Oksøy Fyr
Norway, Group IV

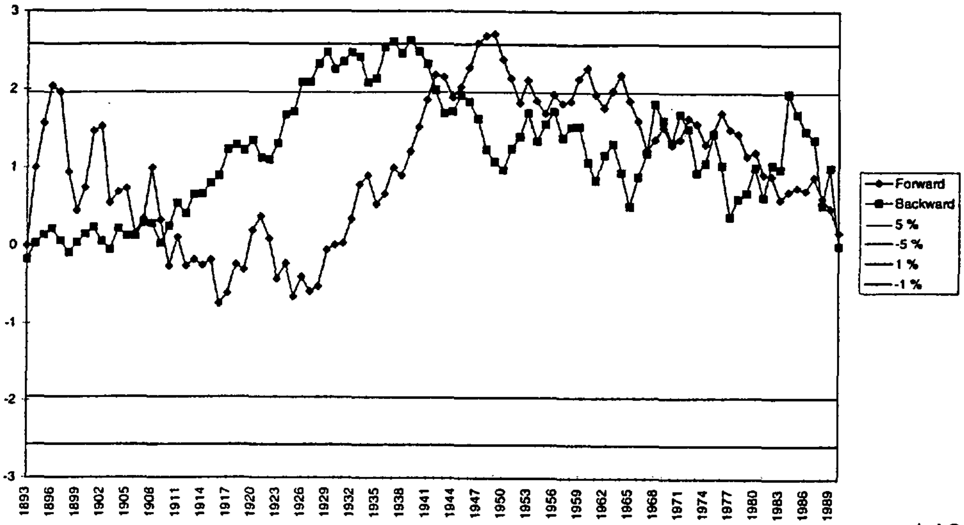

1482 Ferder Fyr
Norway, Group IV

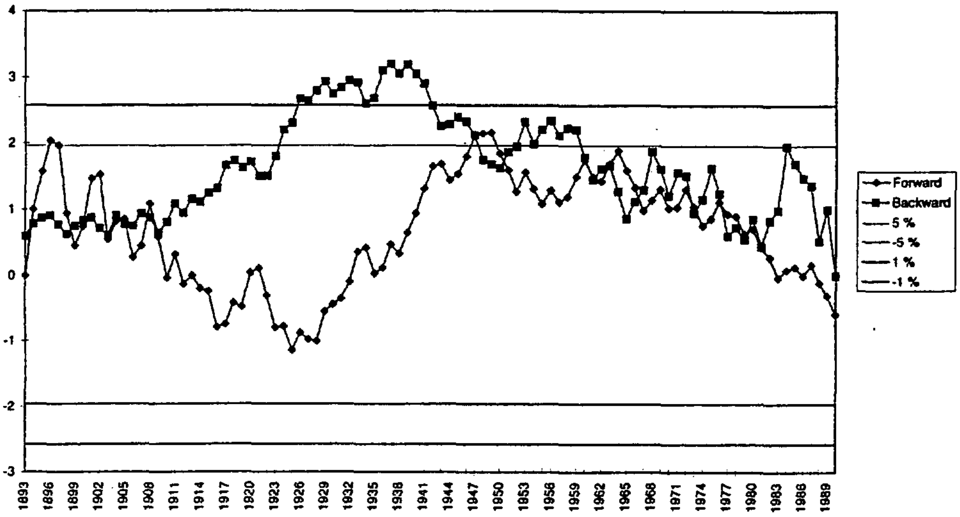

1492 Oslo-Blindern
Norway, Group IV

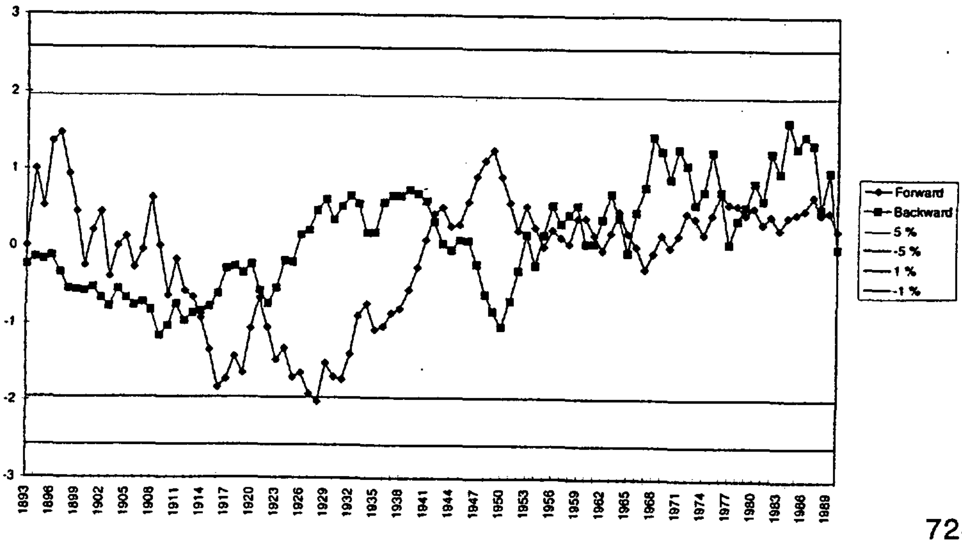

7243 Göteborg
Sweden, Group IV

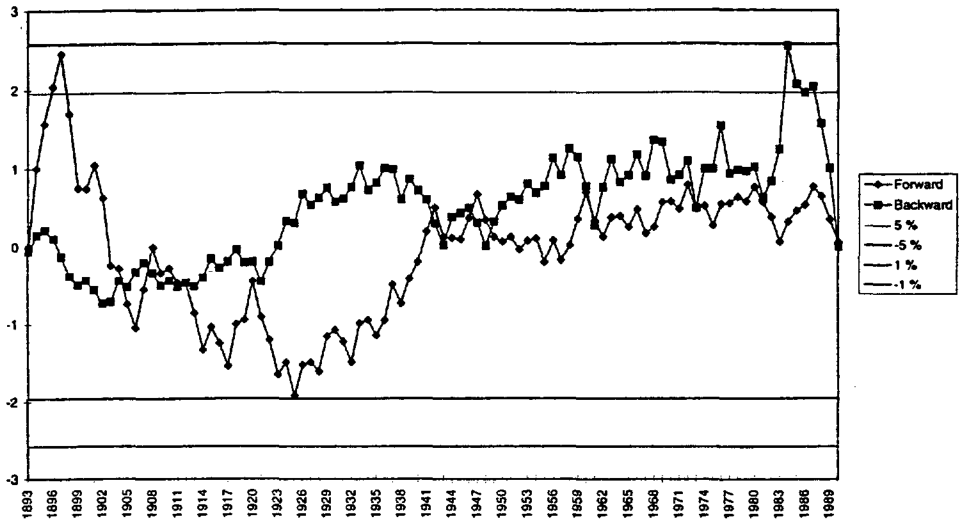

5404 Oulu
Finland, Group VI

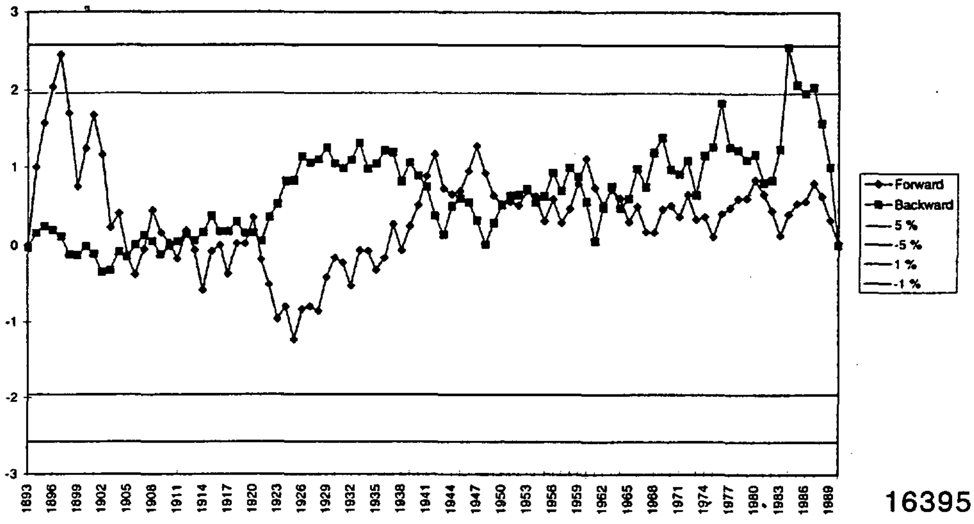

16395 Haparanda
Sweden, Group VI

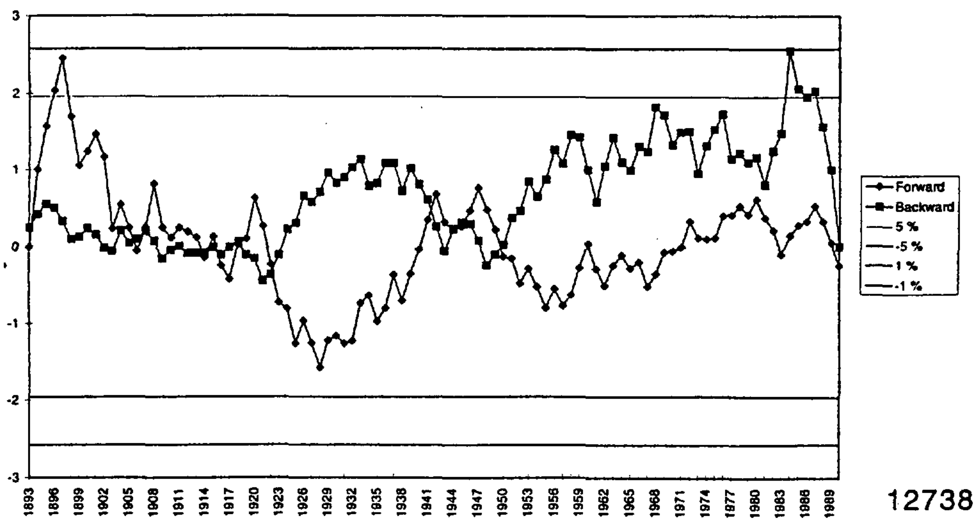

12738 Härnösand
Sweden, Group V

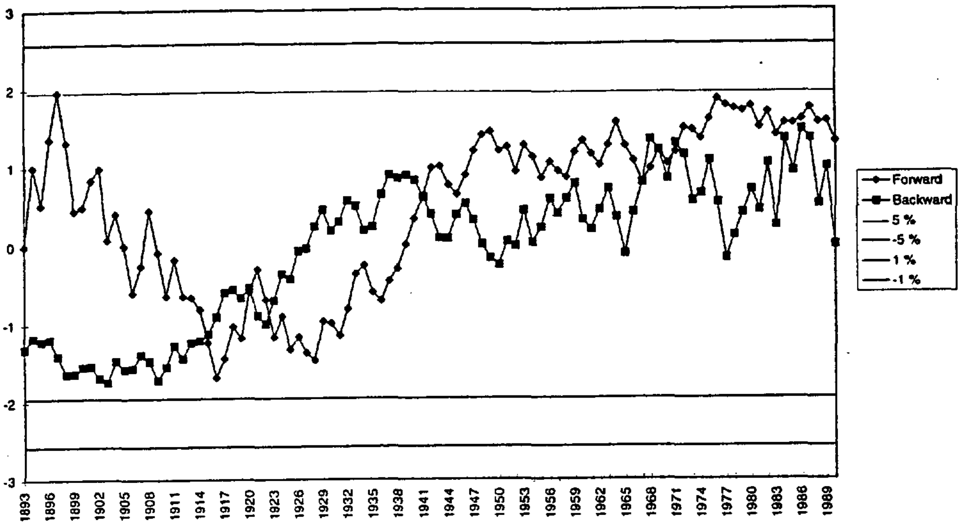

7839 Visby
Sweden, Group V

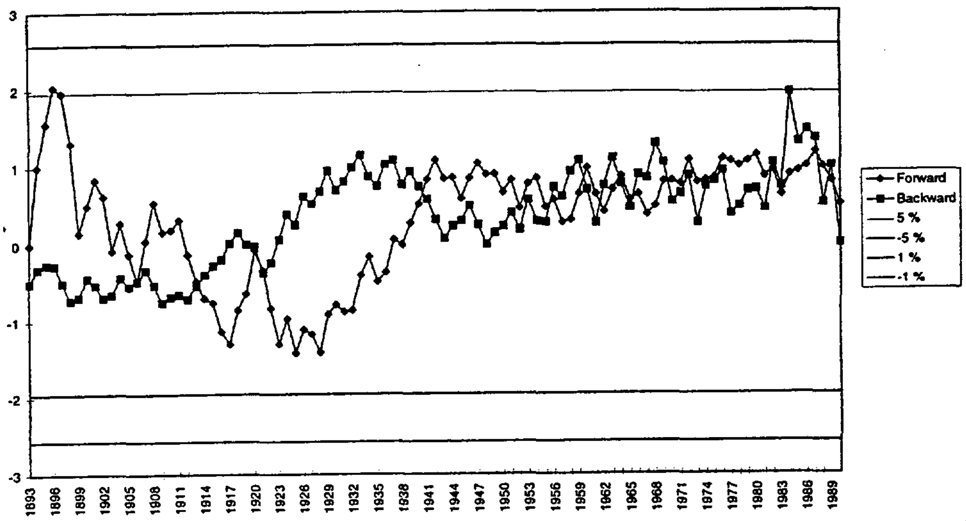

304 Helsinki
Finland, Group V

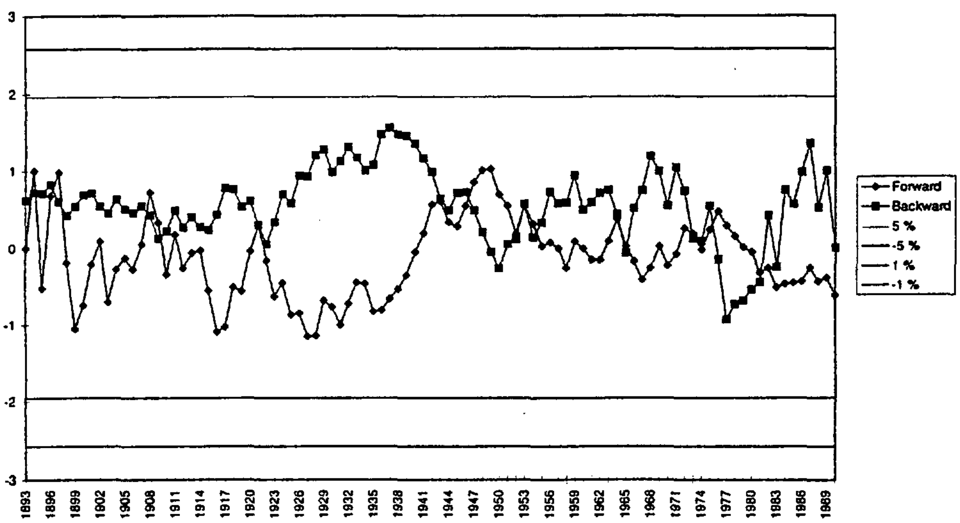

6641 Kalmar
Sweden,Group VII

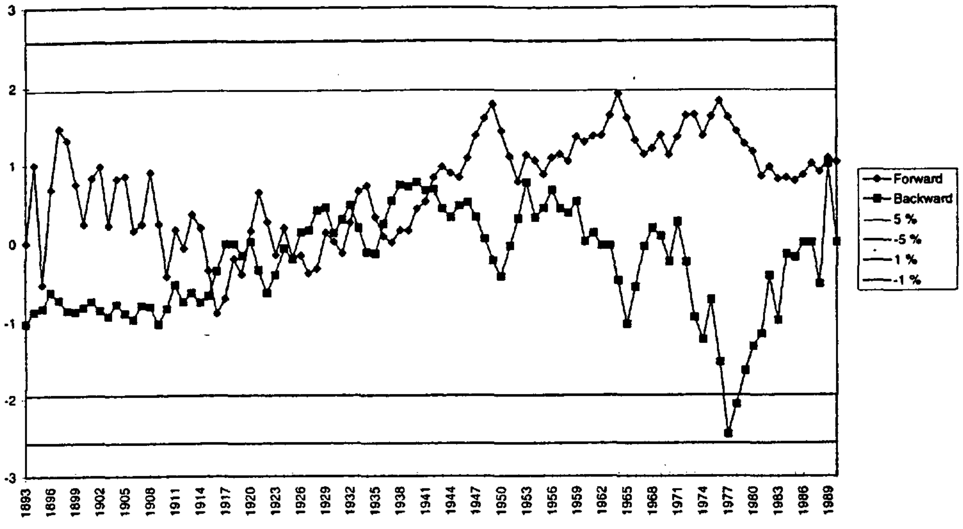

6193 Hammerodde Fyr
Denmark, Group VII

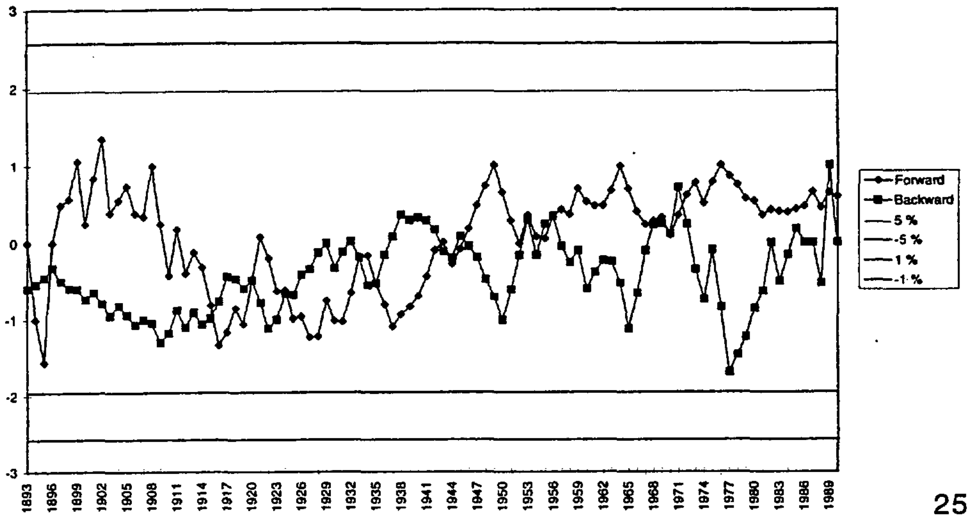

25140 Nordby
Denmark, Group VII

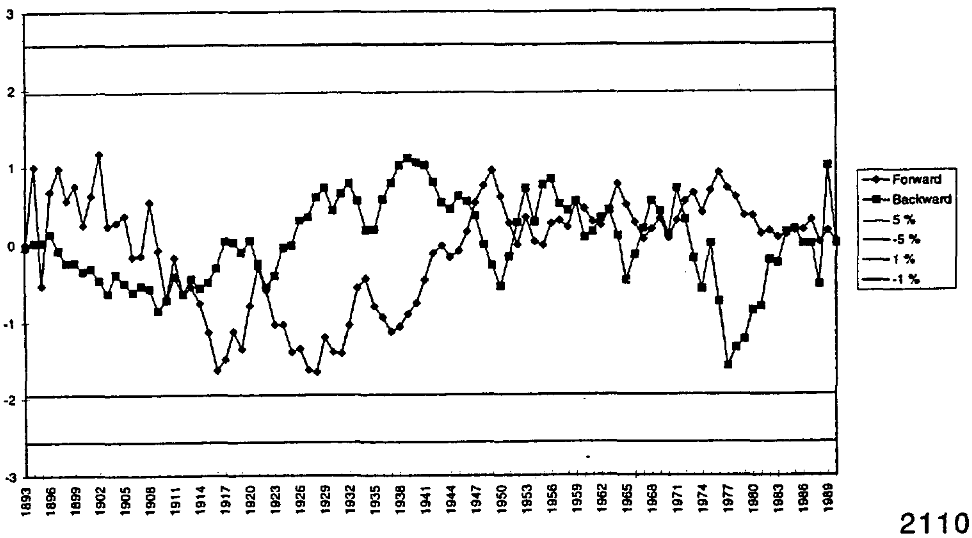

21100 Vestervig
Denmark, Group IV

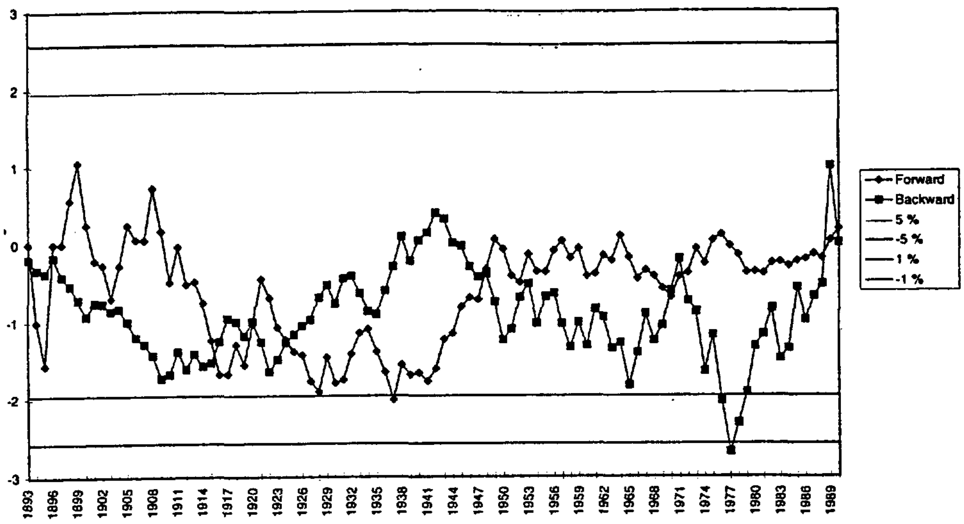

6447 Uccle
Belgium, Group VIII